



# VCU

Virginia Commonwealth University  
VCU Scholars Compass

---

Theses and Dissertations

Graduate School

---

2006

## HMG-CoA Reductase Inhibitors Act Synergistically with UCN-01 Through RAS Inhibition

Payal Khanna  
*Virginia Commonwealth University*

Follow this and additional works at: <https://scholarscompass.vcu.edu/etd>



Part of the [Biomedical Engineering and Bioengineering Commons](#)

© The Author

---

Downloaded from

<https://scholarscompass.vcu.edu/etd/953>

This Thesis is brought to you for free and open access by the Graduate School at VCU Scholars Compass. It has been accepted for inclusion in Theses and Dissertations by an authorized administrator of VCU Scholars Compass. For more information, please contact [libcompass@vcu.edu](mailto:libcompass@vcu.edu).

HMG-CoA REDUCTASE INHIBITORS ACT SYNERGISTICALLY WITH UCN-01  
THROUGH RAS INHIBITION

A thesis submitted in partial fulfillment of the requirements for the degree of Master of Science at Virginia Commonwealth University.

by

PAYAL KHANNA  
Bachelor's of Science, Virginia Commonwealth University, 2002  
Master of Science, Virginia Commonwealth University, 2005

Director: STEVEN GRANT, M.D.  
HEMATOLOGY ONCOLOGY

Director: GARY L. BOWLIN, PH.D.  
BIOMEDICAL ENGINEERING

Virginia Commonwealth University  
Richmond, Virginia  
May 2006

## Acknowledgement

I would like to especially thank Dr. Steven Grant for giving me the opportunity to work with such a diverse group of people. He encouraged me to continue in the pursuit of knowledge and is truly a perfectionist, inspiring me to never settle for anything but the best.

I would also like to thank Dr. Yun Dai and Dr. X-Y Pei for acting as my mentors who spent late hours analyzing my data and refining my knowledge and skills. In addition, I would like to thank Tracy Hamm for her hard work that greatly aided my research. Finally, I would like to thank mother and father, for their unfailing love and guidance. I dedicate this work to them and Dr. Bijan Rao who devoted his life to research in the field of physics and is truly missed.

## Table of Contents

	Page
Acknowledgements.....	ii
List of Figures.....	v
List of Abbreviation.....	7
Chapter	
<b>1 Introduction.....</b>	<b>11</b>
<b>1.1 Mechanism of Cancer Proliferation and Survival.....</b>	<b>11</b>
<b>1.2 Cell Cycle.....</b>	<b>11</b>
<b>1.3 UCN-01 (7-Hydroxystaurosporine).....</b>	<b>14</b>
<b>1.4 Mevalonate Pathway.....</b>	<b>16</b>
<b>1.5 RAS/RAF/MEK/ERK.....</b>	<b>17</b>
<b>1.6 PI3Kinase/ AKT Pathway.....</b>	<b>19</b>
<b>1.7 Crosstalk between RAS/RAF/MEK/ERK and PI3K/AKT.....</b>	<b>20</b>
<b>1.8 Cell Death.....</b>	<b>21</b>
<b>2 MATERIALS and METHODS.....</b>	<b>25</b>
<b>2.1. Cell Culture/Maintenance.....</b>	<b>25</b>
<b>2.2. Determination of Cell Density.....</b>	<b>26</b>
<b>2.3. Cell Viability.....</b>	<b>27</b>
<b>2.4. DNA Amplification and Purification.....</b>	<b>27</b>
<b>2.5 Transfection of DNA into U266 Cells.....</b>	<b>29</b>
<b>2.6 Reagents.....</b>	<b>30</b>
<b>2.7 Experimental Format.....</b>	<b>30</b>

2.8 Analysis of Apoptosis.....	30
2.9 Analysis of Mitochondrial Membrane Potential ( $\Delta\Psi_m$ ).....	31
2.10 Annexin V-FITC Analysis.....	32
2.11 Cell Cycle Analysis.....	33
2.12 DNA Fragmentation.....	34
2.13 Clonegenicity.....	35
2.14 Western Blot Analysis.....	36
2.15 Analysis of Cytochrome C.....	40
2.16 Statistical Analysis.....	40
<b>3 Results and Data Analysis.....</b>	<b>42</b>
<b>3.1 Co-administration of UCN-01 and HMG-CoenzymeA Reductase         Inhibitors Induces a Dramatic Apoptotic Response.....</b>	<b>42</b>
<b>3.2 UCN-01 Combined with Lovastatin Induces PARP Cleavage and         Caspase Activation.....</b>	<b>45</b>
<b>3.3 UCN-01/HMG-CoA Reductase Inhibitors Induce G2/M Abrogation         and Changes in Cell Morphology.....</b>	<b>47</b>
<b>3.4 UCN-01 and Lovastatin Induce Mitochondrial Membrane Damage and         Induces XIAP and Caspase 3 Cleavage.....</b>	<b>49</b>
<b>3.5 Lovastatin Blocks MEK/ERK Pathway Activated by UCN-01.....</b>	<b>49</b>
<b>3.6 Myeloma Cells Show Dramatic Apoptotic Response.....</b>	<b>51</b>
<b>3.7 Mitochondrial Dysfunction and PARP Cleavage.....</b>	<b>54</b>
<b>3.8 Inhibition of RAS in Multiple Myeloma.....</b>	<b>55</b>

<b>4 Discussion and Conclusion.....</b>	<b>57</b>
<b>4.1 Exposure of Leukemia Cells to Low Doses of UCN-01 and Lovastatin         Results in a Dramatic Apoptotic Response.....</b>	<b>57</b>
<b>4.2 UCN-01/Lovastatin Induces Apoptosis Via the Mitochondrial         Pathway.....</b>	<b>57</b>
<b>4.3 Lovastatin Enhances UCN-01 Lethality Through Inactivation of         RAS/RAF/MEK/ERK Pathway in Leukemia and Multiple Myeloma         Cells.....</b>	<b>58</b>
<b>4.4 Conclusion and Further Research.....</b>	<b>60</b>
Literature Cited.....	62

## List of Figures

	Page
Figure 1.1: <b>Cyclin Synthesis and Degradation</b> .....	13
Figure 1.2: <b>Cell Cycle Regulation</b> .....	14
Figure 1.3: <b>Chemical Structure Staurosporine</b> .....	15
Figure 1.4: <b>RAS GTP-Binding Protein</b> .....	19
Figure 1.5: <b>Multiple Mechanisms of Cell Survival Regulation by PI3K/AKT/PKB</b> .....	20
Figure 1.6: <b>PI3K/AKT Pathway and Downstream Targets of RAS</b> .....	21
Figure 3.1: <b>Dose Response for U937 and Jurkat Cells</b> .....	43
Figure 3.2: <b>Dose Response for U937 and Jurkat Cells</b> .....	44
Figure 3.3: <b>Combination Index for Jurkat and U937 Cells (1000:5)</b> .....	45
Figure 3.4: <b>Annexin and Western Blot Analysis</b> .....	46
Figure 3.5: <b>DNA Analysis and Cell Cycle</b> .....	48
Figure 3.6: <b>Western Blots and Cytochrome C Analysis</b> .....	49
Figure 3.7: <b>PI3K/AKT and RAS/RAF/MEK/ERK</b> .....	50
Figure 3.8: <b>Dose Response for MM.IR and 8226 Cells (18 Hours)</b> .....	52
Figure 3.9: <b>Dose Response for MM.IR and 8226 Cells (18 Hours)</b> .....	53
Figure 3.10: <b>Combination Index for MM.IR and 8226 Cells (18 Hours)</b> .....	54
Figure 3.11: <b>Mitochondrial Dysfunction and Annexin V Analysis</b> .....	55
Figure 3.12: <b>RAS Expression in Multiple Myeloma (8226 Sensitive Cells)</b> .....	56

## List of Abbreviations

Acute Myeloid Leukemia	(AML)
Apoptosis-Inducing Factor	(AIF)
Apoptotic protease-Inducing Factor	(Apaf-1)
Chymostatin, Leupeptin, Aprotinin, Pepstatin, and Soybean Trypsin Inhibitor	(CLAPS)
Cleavage Fragment	(CF)
Cytochrome C	(cyt C)
Cyclin-Dependant Kinase	(CDK)
Death Inducing Signaling Complex	(DISC)
3,3-Dihexyloxycarbocyanine Iodide	(DiOC6)
Extracellular Signal-Regulated Kinase	(ERK)
Fetal Bovine Serum	(FBS)
Fluvastatin	(XU)
Histone Deacetylase Inhibitors	(HDACI)
Lovastatin	(LV)
Mitochondrial Membrane Potential	( $\Delta\Psi_m$ )
Mitogen-Activated Protein Kinase	(MAPK)
Simvastatin	(MK)
Phosphatidylinositol-3-Kinase	(PI3K/AKT)
Phosphate Buffered Saline	(PBS)



Phosphorylated Rb Protein	(pRb)
Poly-(ADP-ribose) Polymerase	(PARP)
Propidium Iodide	(PI)
Protein Kinase C	(PKC)
Reactive Oxygen Species	(ROS)
Type 1 Tumor Necrosis Factor	(TNF1)
TNF-Related Apoptosis-Induced Ligand	(TRAIL)
7-Hydroxystaurosporine	(UCN-01)

## Abstract

### HMG-CoA REDUCTASE INHIBITORS ACT SYNERGISTICALLY WITH UCN-01 THROUGH RAS INHIBITION

By Payal Khanna, M.S.

A thesis submitted in partial fulfillment of the requirements for the degree of Master of Science at Virginia Commonwealth University.

Virginia Commonwealth University, 2005

Major Director: Steven Grant, M.D.  
Hematology Oncology

The primary objective of this study is to elucidate the mechanism by which the reagent UCN-01 induces apoptosis when administered to leukemia cells along with HmG-CoA reductase inhibitors, mainly the statins. In this study, we demonstrated that exposure of leukemia cell lines to lovastatin (20  $\mu$ M, 18 hours) and UCN-01 (100 nM, 18 hours) resulted in mitochondrial dysfunction, procaspase 3 and 9 cleavage, and PARP degradation along with marked cytochrome C release and apoptosis. Although similar molecular mechanisms have not yet been confirmed in other cancers, our hypothesis holds that enhanced apoptotic effects of UCN-01 are due in part to lovastatin's ability to block formation of geranylgeranylpyrophosphate and farnesylpyrophosphate by interfering with

the rate-limiting step of the mevalonate pathway. Geranylgeranylpyrophosphate and farnesylpyrophosphate induce post-translational modifications in RAS that anchor the protein to the cell membrane so that it acts as a signal transducer to the nucleus, promoting cell proliferation.

# INTRODUCTION

## 1.1 Mechanisms of Cancer Proliferation and Survival

Hematopoietic cells originate from common stem cells, which have pluripotent function and give rise to two types of progenitors, B lymphocytes and T lymphocytes or leukocytes and erythrocytes. The process of continual hematopoietic proliferation and differentiation of cells is balanced physiologically through apoptotic or mechanisms that induce cell death. Cancers including leukemia and multiple myeloma are due in part to errors existing in genetic code within immature hematopoietic cells resulting in abnormal expression of proteins and evasion of cell death, hindering cell maturity. Most chemotherapies target the specific pathways that initiate inappropriate protein expression in cancer cells in an attempt to induce apoptosis.

## 1.2 Cell Cycle

Several transforming mutations involving RAS/RAF/MEK/ERK and PI3K/AKT pathways have been linked to cell cycle arrest or inappropriate activation of CDKs thus it is important to study the underlying mechanisms that control the transition of the cell from one stage to the next. Cells proceed through five phases: the S, G1, G2, M, and Go. In the Go phase, terminally differentiated cells withdraw from the cycle. Once extracellular signals commit the cells to entry in the G1 phase, RNA and protein synthesis prepare the cell to divide, cells passing a restriction point are therefore committed to entry into the S

phase. The transition of the G1 to S phase is tightly controlled by protein kinases that change their conformation in response to extracellular signals. Protein kinases phosphorylate specific proteins at specific times to coordinate metabolic activities and initiate orderly cell division, consisting of a regulatory (cyclin) and a catalytic (CDK) subunit. When cyclin binds, the catalytic site opens and activity of the CDK increases 10,000 fold. There are several forms of cyclin/CDK complexes corresponding to the transition of each stage of the cell cycle. During the first phase of the cycle, the G1 phase, cyclin D forms a complex with the CDK4 or CDK 6 subunit. Once cyclin D associates with CDK4 or 6, phosphatase Cdc25C acts as a checkpoint control to DNA damage in the S phase. This CDK complex then phosphorylates the protein Rb, which is a tumor suppressor protein involved in sequestration of E2F transcription factors that prevent activation of genes critical for DNA synthesis during the S phase. Once Rb is phosphorylated, E2F transcription factors are expressed, allowing DNA synthesis during the S phase. In several studies, overexpression of cyclin D or loss of Rb function has been linked to tumors. Late in G1, cyclin E forms a complex with CDK2 and this marks the entry of the cell into the S phase. The synthesis of cyclin E promotes the synthesis of additional E2F transcription factors, thus, this process acts a positive feedback loop. Once in the S phase, cyclin E is degraded and CDK2 associates with cyclin A and B, allowing the cell to enter mitosis and undergo cell division. Progress through mitosis requires that there is timed activation and then destruction of cyclins A and B, which activate CDK2. Continual synthesis and degradation of cyclins allow their counterpart, CDKs to become activated at appropriate times, followed by inactivation.

As illustrated in Figure 1.1, production of cyclins followed by their degradation allows for transitioning of the cell from one phase to the next, while CDK levels remain fairly constant. These CDKs are tightly controlled and depend on association with cyclins followed by inactivation of CDKs through action of anti-growth factors and CDK inhibitors belonging to either Cip/Kip family or CDK4 inhibitors. Members of the Kip family include p21, p27, and p57 and may inhibit CDK 2, 4, and 6.

**Figure 1.1 Cyclin Synthesis and Degradation (18)**

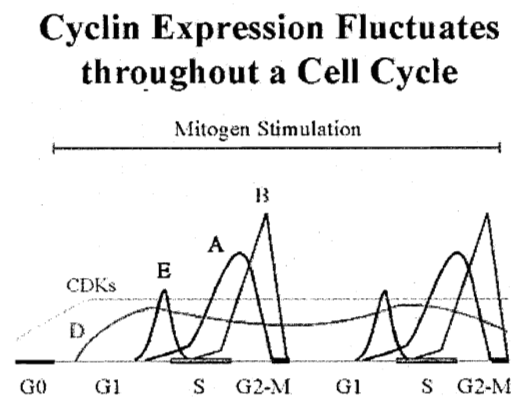
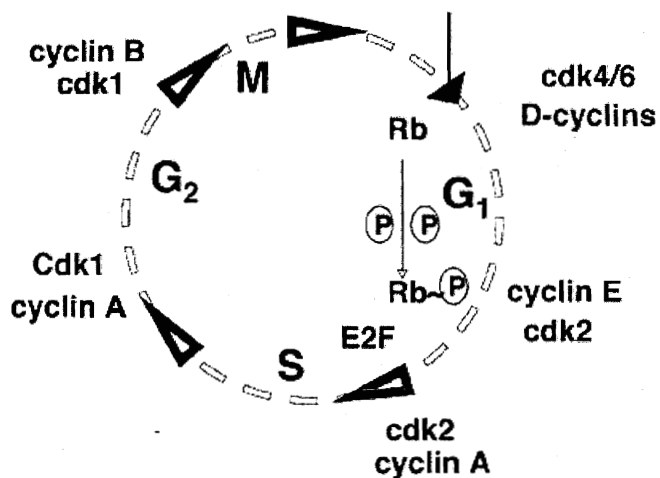


Figure 1.2 illustrates the corresponding cyclin-CDK complexes that regulate the cell cycle. In several tumors, inappropriate activation of CDKs has caused cell proliferation in the absence of extracellular signals such as hormones. There have been several synthetic inhibitors created that modulate CDK activity to induce apoptosis, causing cell cycle arrest in an attempt to counteract continual cell proliferation brought about by cancer. Most of these inhibitors act via interaction with the ATP site of cdk's, these inhibitors include

UCN-01, flavopiridol, and roscovitine. In this study, the major CDK inhibitor was 7-hydroxystaurosporine, an analog of UCN-01.

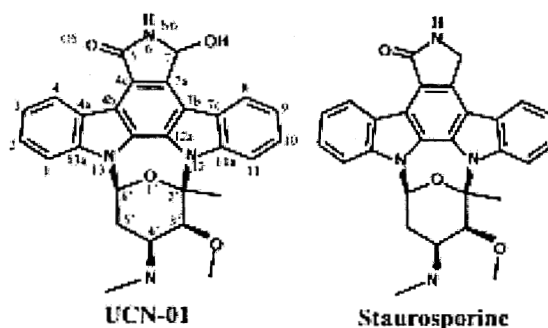
**Figure 1.2 Cell Cycle Regulation (18)**



### 1.3 UCN-01 (7-Hydroxystaurosporine)

7-hydroxystaurosporine has been classified as a specific analogue of staurosporine that specifically targets protein kinases (24). UCN-01 specifically inhibits protein kinase C isoenzymes, specifically those isoforms that are calcium dependant. The reagent has a hydroxyl group at the C-7 position of the indolocarbazolo moiety with the following structure.

**Figure 1.3: Chemical Structure: Staurosporine (28)**



Although it is apparent in some tumors that UCN-01 acts via targeting of PKC enzymes; other tumors treated with UCN-01 indicate an alternate mechanism of action (12). One theory is that UCN-01 induces inhibition of CDKs at high concentrations *in vitro*, while S-G1 arrest was observed at lower concentrations. In the most recent studies on the effects of UCN-01 on cell cycle control, upregulation of the protein p21 was observed, which as mentioned previously is involved in deactivation of CDKs and subsequent cell cycle arrest. Since p21 has similar promoter regions to those existing in the proto-oncogene protein RAS, which activates p21, scientists have studied the effects of UCN-01 on other kinases activated by the protein RAS including MEK/ERK have been investigated.

Previously, it has been found that at concentrations  $\geq 100$  nM, UCN-01 significantly increases ERK activity and similar concentrations were found to increase activation of MAPK, another pathway regulated by RAS. Thus, the increased activity of p21 is due to increased activation of MEK/ERK and MAPK leading to observed cell cycle arrest. Although these studies aid understanding of the mechanism involved in apoptosis



when cells are exposed to UCN-01 alone, the apoptotic effects are minimal. In this study, UCN-01 was used at lower concentrations (100-150 nM) in combination with other inhibitors. In our studies, it was discovered that UCN-01 in combination with farnesyltransferase inhibitors (LY744), caused G2/M abrogation, while interfering with UCN-01 induced activation of the MEK/ERK pathway.

#### **1.4 Mevalonate Pathway**

In the past, statins have mainly been involved in control of cholesterol where their mechanism of action has been to block an essential component of the mevalonate pathway (18). Here, the rate-limiting step of the pathway is conversion of HMG-CoA to mevalonate, which then leads to products, which have various functions within the cell. The products contain isoprene units and include GGPP (geranylgeranyl pyrophosphate), FPP (farnesyl pyrophosphate), and cholesterol. Geranylgeranyl and farnesyl transferases use the substrates, GGPP and FPP to perform post-translational modifications to GTP-binding proteins so that they may function, these proteins include RAS and other proteins belonging to families Rho, Rac, etc. (2). For RAS to act as a signal transducer the protein must be localized to the cytosolic face of the membrane, which occurs by attaching hydrocarbon moieties to the existing protein. In this case, RAS is anchored to the membrane by two such moieties, either farnesyl or geranylgeranyl hydrocarbons. The bond between the farnesyl or geranylgeranyl group and RAS protein is a thioester linkage, which is formed with the cysteine group close to the carboxyl terminus of the protein and the hydrogen on the farnesyl or geranylgeranyl moiety. Following modification of RAS, the protein undergoes proteolysis in which three of the terminal residues of the protein are

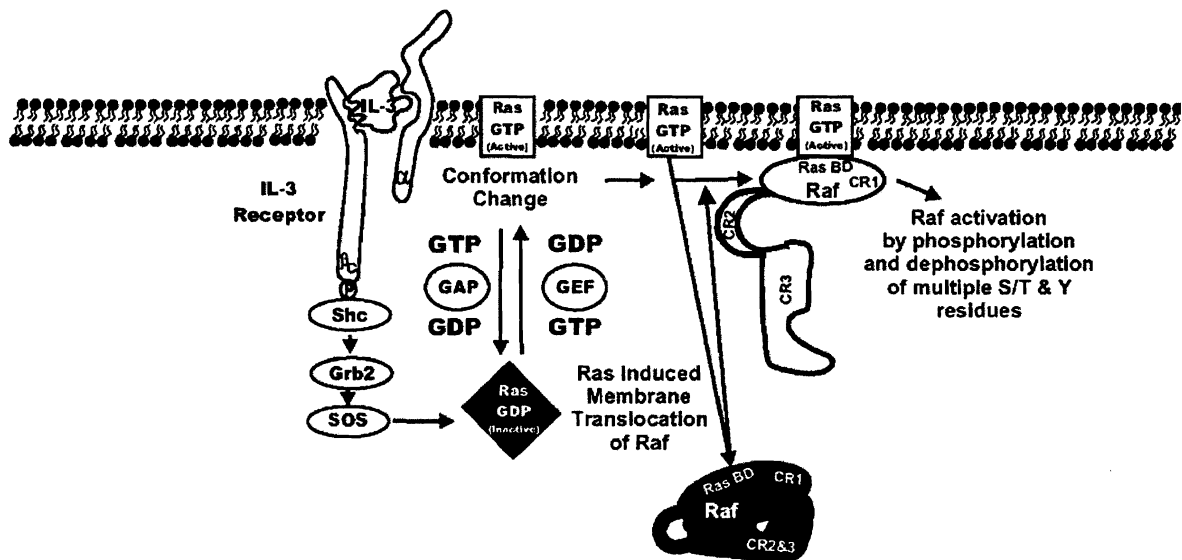
removed and the carboxy terminus is methylated. The transfer of the farnesyl moiety required for the above reaction is catalyzed by the enzyme farnesyltransferase, which interacts with the substrates produced by the mevalonate pathway, FPP (farnesylpyrophosphate) and GGPP (geranylgeranylpyrophosphate). As previously reported inhibition of farnesyltransferase inhibits localization of the RAS protein to the cell membrane, and subsequent activation of downstream signaling pathways. The lethality of farnesyl transferase inhibitors were enhanced when combined with UCN-01. However, RAS isoforms may still overcome the effects of these inhibitors since geranylgeranyl moieties also bind particular members of the RAS family, including HRAS and NRAS to the cell membrane. As mentioned above, blocking RAS may dramatically enhance the effects of the CDK inhibitor, UCN-01 (4). One of the theoretical advantages of using HMG- CoA reductase inhibitors is the tolerance exhibited by patients of side-effects and decreases in the amount of FPP and GGPP produced, which are required for farnesyltransferase to function and to modify RAS. Generally, there are four different forms of statins. Fluvastatin and atorvastatin are synthetically derived whereas simvastatin and lovastatin are fungal derivatives (2). In this study, we are primarily concerned with three forms of the drug: Lovastatin, simvastatin, and fluvastatin and their actions when combined with UCN-01.

### **1.5 RAS/RAF/MEK/ERK**

The RAS/RAF/MEK/ERK pathway is often referred to the MAP kinase pathway or mitogen-activated protein kinase. The pathway is stimulated by a variety of factors

including activation of growth factors, cytokines, and mitogens responsible for cell division and induction of mitosis initiated by factors in the extracellular medium. In cancer, the MEK/ERK pathway is activated by RAS in the absence of growth factors or hormones, RAS subsequently promotes the translocation of RAF-1 from the cytosol to the cell membrane, and RAF is then activated by phosphorylation and dephosphorylation. RAS is a small GTP-binding protein that is activated by binding to GTPase activating proteins and guanine nucleotide exchange factors. RAS will cycle between the active form, which is bound to GTP and the inactive state, bound to GDP for short periods of time. In cancers, RAS bound to GTP is hydrolyzed in its active state for an abnormally long period of time accumulating growth-promoting signals sent to the nucleus in the absence of growth factors or hormones, in turn, activating the MAPKinase cascade described later in this section. There are several family members of RAS protein including HRAS, KRAS, and NRAS. The major isoforms found in almost 30 percent of cancers include KRAS and NRAS. RAS not only activates RAF-1 and the MEK/ERK kinases, it is the major regulator of the survival pathway, PI3K/AKT.

Figure 1.4 RAS GTP-Binding Protein (34)



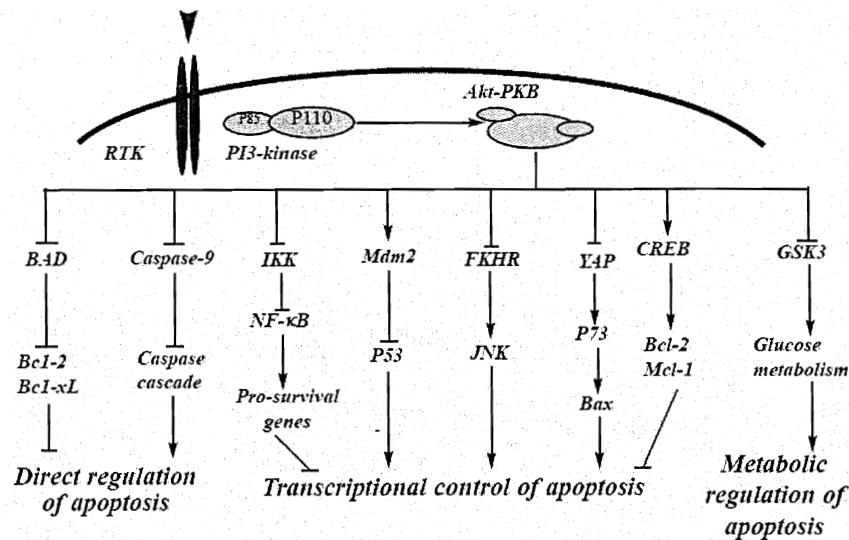
## 1.6 PI3K/AKT Pathway

The PI3K/AKT survival pathway is one of several pathways involved in cell cycle regulation as mentioned previously. Specifically, PI3K/AKT is responsible for phosphorylation of T145 and S146 near the carboxyl terminus of p21 leading to activation of CDK and DNA synthesis and an increase in cell proliferation (3).

The PI3K/AKT pathway is activated via cytokine activity for specific receptors that activate PI3 Kinase. The exact mechanism, by which PI3K/AKT is activated, occurs when PI3K is recruited to the plasma membrane and is phosphorylated at Thr308 by PDK1 and at Ser473 by PDK2. PP2A is a serine/threonine-specific phosphatase that has been shown to inhibit PI3K/AKT kinase activity. Thus, PDK1/PDK2-mediated phosphorylation at both sites and PP2A-mediated dephosphorylation must work in conjunction to mediate the PI3K/AKT kinase activity in vivo (3). PI3K/AKT then mediates several cellular responses

such as glucose uptake and several downstream anti-apoptotic proteins including those involved in the mitochondrial pathway such as Bcl-xl and Bcl-2. The following Figure illustrates several mechanisms of survival for the PI3K/AKT pathway.

**Figure 1.5 Multiple Mechanisms of Cell Survival Regulation by PI3K/AKT/PKB (3)**



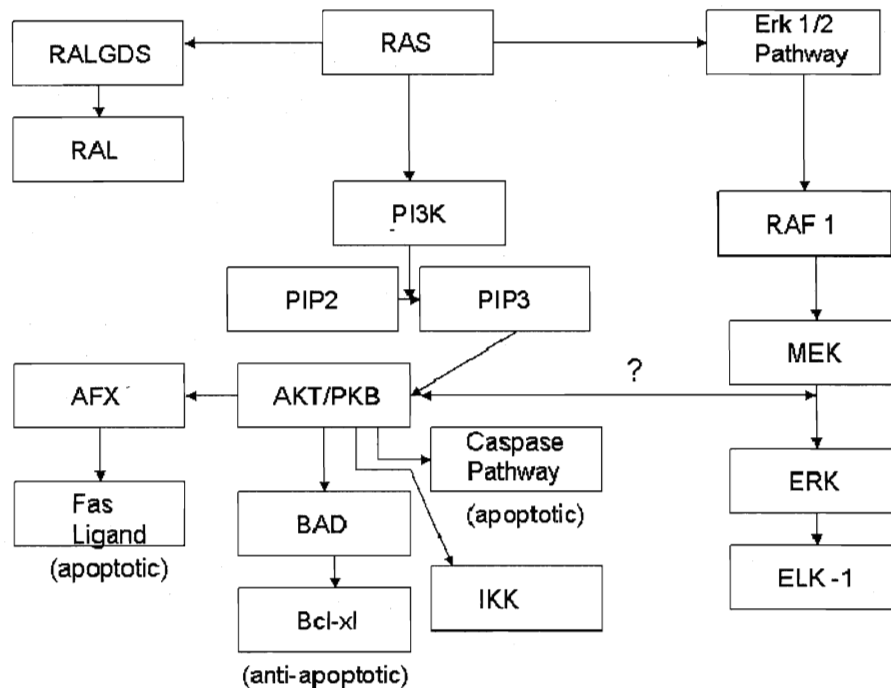
Another mechanism by which PI3K/AKT suppresses apoptosis is through inhibition of apoptotic proteins belonging to the caspase family of cytosolic proteases (5). Reports indicate that suppressing the PI3K/AKT pathway with PI3 Kinase inhibitors such as LY294002 (farnesyltransferase inhibitors) synergistically enhances the cytotoxic effects of anticancer drugs such as UCN-01.

### 1.7 Crosstalk Between RAS/RAF/MEK/ERK and PI3K/AKT

Although RAS regulates several pathways including PI3K/AKT, ERK 1/2, and the Ral GDS pathways, recently it has been found that crosstalk between PI3K/AKT and RAF may occur since PI3K/AKT can directly phosphorylate RAF isoforms, however these effects depend on the cell type and differentiation process. The first indication of possible

crossstalk between the pathways was evident when inhibition of PI3K/AKT was shown to cause a marked decrease in the amount of expression of p-ERK. In previous studies it has been demonstrated that farnesyltransferase inhibitors such as LY294002 that inhibit PI3K/AKT also induce expression of B-RAF. Such findings warrant further study as to the exact interaction between the PI3K/AKT and RAF pathway.

**Figure 1.6 PI3K/AKT Pathway and Downstream Targets of RAS**



## 1.8 Cell Death

Although there are several pathways which promote cell survival, these mechanisms must be balanced physiologically through apoptosis or cell death. Cell death occurs via two mechanisms: necrosis or apoptosis. Necrosis is a pathological process of

cell death in living organism with failure of membrane integrity. The cell membrane and membranous structures within the cell become permeable as opposed to their normal physiological state. A number of toxic chemicals or physical events can cause necrosis including toxins, radiation, heat, trauma, or lack of oxygen. This process follows cell injury and the resulting dead cells induce an inflammatory response. Necrosis is distinguished from apoptosis in that apoptotic cell death results from energy dependent, metabolically active, endogenous cellular processes where membrane integrity is maintained.

The induction of apoptosis generally follows one of the two related biochemical pathways, either extrinsic or intrinsic. The extrinsic pathway is initiated by the cell-surface molecules belonging to the tumor necrosis factor (TNF) family of receptors (Fas[DR2], DcR3) and their respective ligands.

Typically, receptors belonging to the TNF form what is known as a death-inducing signal complex or DISC when paired with their respective ligands. Directly following formation of the complex, caspase 8 and caspase 10 proteins are activated, which activate effector proteins caspase 3, 6, and 7 downstream. Caspases are cytosolic proteases that participate in apoptosis when there is a signal from the receptor. All caspases are synthesized as inactive proenzymes and all have a critical cys residue at the active site.

The Fas receptor, a member of the TNF family, induces apoptosis via a mechanism similar to that mentioned above. Apoptotic response is initiated when binding of a cluster of Fas receptors at the plasma membrane results in the recruitment of cytosolic protein,

FADD and formation of the pro-caspase 8 complex. High concentrations of the cytosolic proteasome, pro-caspase 8 results in its autocatalysis or self-activation; activated caspase 8 cleaves effector, pro-caspase 3, which then undergoes autocatalysis to form active caspase 3, a principle effector caspase of apoptosis.

One area of interest in cancer research has been the TNF-related apoptosis-induced ligand (TRAIL) and its receptor, which has shown great promise as an anticancer reagent. TRAIL derivatives have been shown to induce apoptosis in tumor cells, while rarely inducing apoptotic responses in non-transformed cells. However, the exact molecular mechanism is not well understood. In contrast to Fas, TRAIL expression has been found in numerous tissues including the spleen, thymus, and ovary, but is absent in the brain (20). There are structural similarities between TRAIL and other TNF receptors; both are type II transmembrane proteins expressed on the cell surface. Studies indicate that TNF receptors contain a specific group of molecules on the receptor that are responsible for inducing apoptosis; these four molecules include TNFR1, CD95, DR3, and CAR1. Each of these molecules contain a “death domain”, an 80 amino acid cytoplasmic motif, which form a complex with the “death domain” on the ligand to activate the caspase cascade and induce apoptosis. However, experimentation indicates that receptors lacking this domain still retain the ability to mediate apoptosis in T-cells, indicating a more complex mechanism which warrants further molecular studies to elucidate the exact mechanism.

The other major signaling pathway is the intrinsic pathway also known as the mitochondrial pathway and is activated via mitochondrial membrane damage and may be



triggered from within the cell as opposed to the ligand-receptor system involved in the extrinsic pathway. Apoptosis through this mechanism is detected through release of a carrier protein, cytochrome C, from damaged mitochondria that binds a protein, Apaf1. This cascade of events initiates caspase 9 that activates effector caspase 3. A delicate balance exists in which apoptotic proteins such as SMAC/DIABLO and Omi/HtrA2, which are released from the mitochondria, may inhibit the action of anti-apoptotic proteins such as Bcl-2 and XIAP. The common protein that links the extrinsic and intrinsic pathways is caspase 3 whereas several anti-apoptotic proteins such as XIAP target effector caspase 3 and 7, preventing apoptosis.

In summary, several major pathways exist that promote cell survival including PI3K/AKT and MEK/ERK, both of which are activated by the protein RAS. These pathways are complex and influence cell cycle activity. In addition, these survival pathways influence apoptotic responses brought about by the caspase cascade, which may be triggered within the cell or via the extrinsic pathway. In this study, the PKC and Chk1 inhibitor UCN-01 was administered at low concentrations (100-150 nM) in conjunction with HMG-CoA reductase inhibitors in an attempt to induce dramatic apoptosis in leukemia cells lines and define the exact molecular mechanism involved in this response.

## Materials and Methods

### 2.1 Cell Culture/Maintenance

Human Cell Lines: 8226/Sensitive, 1R M.M., U266, U937, and Jurkat are multiple myeloma-sensitive, multiple myeloma, histiocytic lymphoma, acute promyelocytic leukemia, and acute T-cell lines, respectively obtained from American Type Culture Collection (Rockville, MD). Cells were maintained in 1640 RPMI Gibco medium containing 2mM  $C_5H_{10}N_2O_3$  (L-glutamine), 2 grams  $NaHCO_3$ , 10 ug/ml of penicillin, 1 mM  $C_3H_3NaO_3$ , 100 uM MEM nonessential amino acids, and 100 ug/ml streptomycin supplied by Gibco in powder form and dissolved in 1 liter ultrapure water. The pH of the resulting medium was adjusted to 7.25 using NaOH or HCl according to readings from an Omega pH meter. The medium was sterilized using vacuum filtration through a 0.22  $\mu$  filter unit from Pall (Bridgeport, NJ). The bottles of medium were stored at 4°C. Prior to use medium was supplemented with 50 ml of FBS (fetal bovine serum). Cells were incubated in a Greiner T-25 cm<sup>2</sup> flask from ISC Bioexpress in a humidified incubator at 37°C and 5% CO<sub>2</sub>. Once cells were obtained from American Culture Collection, the vial of cells was thawed and cultured (free-floating) in approximately 10 ml of medium for approximately 2-3 days. Once the cells reached a density of approximately  $3 - 5 \times 10^5$  cells/ml, a volume of 0.5 ml cells were taken from the T-25 cm<sup>2</sup> flask and placed in 10-12, 1 ml cryovials containing 0.5 ml Cryo solution (Sigma-Aldrich), were frozen and stored in a liquid nitrogen tank. Cells stored in the nitrogen cryogenic storage vessel were used as needed for experimentation. One cryovial containing cells was thawed and washed 2-3 times in 1 ml of Gibco medium to remove DMSO (see above for contents). Cells

resuspended in 1 ml of medium were added to a T-25 cm<sup>2</sup> flask already containing approximately 10 ml of Gibco medium. Cells were incubated starting from passage number 3 to 60, in a humidified incubator at 37°C and 5% CO<sub>2</sub>. For these cell lines no additional drugs or reagents were added when maintaining cell culture.

## **2.2 Determination of Cell Density**

In order to maintain the cell density between  $3 - 5 \times 10^5$  cells/ml, a coulter Z2 particle counter from Beckman Coulter (Fullerton, CA) was used to determine the density of cells in 1 ml of fluid. The coulter counts the amount of particles passing through the aperture based on the particle size, which is 6  $\mu$ m to 8  $\mu$ m for cells. Smaller cell sizes indicate shrinkage, fragmentation and corresponding cell death. To determine the cell density, a 500  $\mu$ L volume of each cell line maintained was obtained from the flask of growing cells and diluted in 1 ml of conductive fluid obtained from Beckman Coulter. The dilution was thoroughly mixed and then passed through a cylindrical aperture on the coulter Z2 particle counter from Beckman Coulter (Fullerton, CA) that modulates impedance of two electrodes positioned on either side of the apparatus every time a particle passes through the aperture. As each particle passes through the aperture, the circuit is interrupted and an electrical pulse is sent through the circuit, in this case the particles passing through the aperture are cells. The number of electrical pulses corresponds to the number of cells and this number is then illustrated as a peaked curve on a liquid crystal display along with a numerical value on the bottom of the display. This value indicates to the user the number of cells in 1 ml of conductive fluid or concentration of cells. In this case, the range of particle sizes may be specified by the user so that the window displays

particles that range in size from 6um to 8 um, which are the typical sizes for living myeloma and leukemia cell lines. To assess cell viability or for a more precise indication of cell viability trypan blue analysis is used in cases where inconsistent cell growth is indicated or there is discoloration of the medium during cell culture.

### **2.3 Cell Viability**

Trypan blue is one method by which cell viability may be evaluated using a system of scoring of four separate fields on a prepared hemocytometer (Sigma -Aldrich). First 100 uL of cells were taken from the T-25 cm<sup>2</sup> flask and placed in a 0.5 ml microfuge tubes. Then 100 uL of 0.4% trypan blue solution (Sigma-Aldrich) was resuspended in the microfuge tube. The suspension of cells and trypan blue stain was then injected into the hemocytometer (Sigma Aldrich). Cells in all four fields were counted and the number of cells that lacked stain was determined accordingly. Living cells would lack stain since their membranes are in tact, whereas cells with blue stain are damaged due to incorporation of the stain into the cell because of membrane damage.

### **2.4 DNA Amplification and Purification**

DNA purification is used so that DNA may efficiently be transfected in eukaryotic cells. DNA HRas plasmid was ordered from Upstate Biotechnologies and propagated in a DH1 e-coli host strain. The bacterial colonies were grown in a 1.5 % prepared agar plate (agar from Invitrogen) with 50 ug/ml of ampicillan. Once bacterial colonies were visible, a single colony was picked from the prepared agar plate and inoculated in 2-10 ml of Luria Bertani (LB) medium from Qiagen (1 L contains 10 grams NaCl, 10 grams tryptone, 5 grams yeast, and 800 ml ultrapure water). The final pH of the medium was adjusted to 7.0

by adding NaOH, and HCl. The inoculated bacterial culture was incubated for approximately 8 hours at 37°C and shaken at 3000 rpm in a Lab-Line incubator/shaker. The starter culture was further diluted in 500 ml of selective LB medium for every 1 ml of the starter culture. The above procedure was repeated this time for 12 – 16 hours, the bacterial cells in LB medium were then harvested by centrifugation at 6000 x g at 4°C using a Jouan, Model CT 4 22 centrifuge for approximately fifteen minutes and the suspension was aspirated to obtain a pellet of bacterial cells. Purification of the resulting pellet was performed using an Endotoxin Free kit from Qiagen. The bacterial pellet was isolated and then resuspended in 10 ml of P1 Buffer. 1L of P1 contains 6.06 grams of Tris base obtained from BioRad Companies, 3.72 grams Na<sub>2</sub>EDTA, and 100 mg RNase in ultrapure water. The P1 buffer pH was adjusted to 8.0 using NaOH and HCl. Then 10 ml of P2 buffer was added to the suspension and the resulting mixture was incubated at room temperature for five minutes. 1 liter of P2 buffer contains 8 grams NaOH, 50 ml of 20% SDS, and ultrapure water to a final volume of 1 liter. The resulting lysate was viscous and contained contaminants; these impurities were removed via filtration through a qiagen filter cartridge as instructed by the Qiagen supplier. The resulting eluate was collected in pyrogen-free tubes provided by Qiagen. DNA was then precipitated using 10.5 ml of isopropanol warmed to room temperature. The suspension was then mixed and centrifuged at 15000 x g for approximately 30 minutes at 4°C (Jouan, Model CT 4 22) in a 50 ml conical tube. The supernatant was removed and the resulting pellet was resuspended in 5 ml of ethanol. The resulting suspension was centrifuged again at 15000 x g for approximately 10 minutes at 4°C, the suspension was aspirated and the resulting pellet was

dried in air at room temperature. The pellet was then resuspended in 10 uL endotoxin buffer-TE provided by Qiagen. 1 liter of TE buffer contains 5.84 grams NaCl, 1.21 grams Tris base, and 0.37 grams Na<sub>2</sub>EDTA in ultrapure water to a final volume of 1 liter and pH of 8.0.

## **2.5 Transfection of DNA into U266 Cells**

In order to transfect the purified DNA, first U266 cell lines were adjusted to a density of  $3-5 \times 10^5$  cells per ml and the density was confirmed using the coulter Z2 particle counter from BeckmanCoulter (Fullerton, CA). Then 1 ug of DNA obtained from the procedure in section 2.4 was prepared in 5 uL of ultrapure water. A 12 well plate from Nunclon Surface Technologies was then filled with 1.5 ml of 1640 RPMI medium to each well (see section 2.1 for contents). Next, U266 cells were centrifuged in a 50 ml conical tube at 90 x g for 10 min in a Jouan, Model CT 4 22 centrifuge. The supernatant was discarded and the resulting pellet of U266 cells were resuspended in Cell Line Nucleofactor solution warmed to room temperature for approximately 20 minutes (Amaxa Biosystems, Koln, Germany). Then the 1 ug of DNA in ultrapure water was added to the prepared suspension of U266 cells in nucleofactor solution. Then 500 uL of suspension consisting of cells and DNA was transferred to an amaxa cuvette and the sample was placed into a Nucleofactor I system from Amaxa Biosystems (Koln, Germany). In this case, we used nucleofactor technology; program V-01, which was preset by Amaxa Biosystems. Once transfection of U266 cells was complete, 500 uL of pre-warmed 1640 RPMI culture medium was added to the cuvette and 500 uL of U266 cells in medium with the new DNA was transferred to each well in the prepared plate. The 12 well plate was

incubated in a humidified incubator at a temperature of 37°C/ 5% CO<sub>2</sub> for approximately 24 hours to ensure peak expression of the HRas gene. Expression of the gene was confirmed using western blot analysis described in the later sections.

## **2.6 Reagents**

UCN-01 was obtained from the National Cancer Institute from Dr. Edward Sausville. UCN-01 was dissolved in sterile DMSO and frozen under light-protective conditions at -20°C (5). Lovastatin, Simvastatin, and Fluvastatin were purchased from Calbiochem (San Diego, CA). The lovastatin, simvastatin, and fluvastatin were dissolved in DMSO solution and stored at -80 °C in light-protective 1 ml microfuge tubes. Prior to use appropriate dilutions were made for all experiments with sterile DMSO.

## **2.7 Experimental Format**

Experiments were conducted using sterile 6 or 12 well plates obtained from Nunclon Surface. For each experiment a volume of 1000 uL of logarithmically growing cells at a density of approximately  $3-5 \times 10^5$  cells/ml were added to each well. Cells were then treated with UCN-01, Coenzyme reductase inhibitors (Calbiochem San Diego, CA) or a combination of these and incubated at a temperature of 37 °C/ 5% CO<sub>2</sub> at various time intervals, generally intervals of 18 or 36 hours. After treatment, cells were subjected to analysis to determine the extent of apoptosis using the following techniques.

## **2.8 Analysis of Apoptosis**

The extent of apoptosis was first determined by viewing slides prepared by cytospin in a Cyto-Tek centrifuge made by Sakura Finetek for 10 minutes at a speed of 5 rpm. The slides were encased in a filter cartridge with filters obtained from Cyto-Tek.

Approximately 3000 uL of cells were used in each cartridge. Once centrifuged, the slides were stained with Wright-Giemsa stain preparation (Sigma-Aldrich) and viewed under light microscopy using a Zeiss Axiovert 40 x CFL microscope. "Scoring" was performed by approximation of the number of cells that exhibited classical morphological features of apoptosis including condensed nuclei and membrane damage (5). For each condition, 4 or 5 randomly selected fields were evaluated, containing at least 500 cells (5). To confirm the results of morphological analysis, in some cases cells were also evaluated by oligonucleosomal DNA fragmentation of total DNA as described later in this section.

## **2.9 Analysis of Mitochondrial Membrane Potential ( $\Delta\Psi_m$ )**

Mitochondrial membrane potential is used to characterize cellular apoptosis and also cellular metabolism. The theory behind this assay is based on the electron transport chain and changes in membrane potential. The electron transport system across the inner mitochondrial membrane creates a potential that is greatly reduced when the membrane is damaged as it would occur if the cell was undergoing apoptosis. DiOC6 (3, 3-dihexyloxacarbocyanine iodide) is a cationic fluorescent dye. When there is accumulation of DiOC6, it is an indication of living cells, whereas cells that do not take up the dye are dead cells. In this procedure a volume of 300 to 400 uL of cells are transferred to a Falcon brand polystyrene test tubes (12 x 75 mm). For every 100 uL of cells, 4 uL of DiOC6 prepared stock is added to each sample of cells. The prepared stock consists of 40 uL of DiOC6 in 10 ml of PBS (Molecular Probes Inc., Eugene, OR). Once cells were treated with DiOC6 dye, cells were incubated at 37°C/5% CO<sub>2</sub> for 15 min and then analyzed by flow cytometry using a Becton Dickinson FACScan and Cell Quest Pro Software version



4.1 (Becton Dickinson, San Jose, CA). FacScan channels F1-1 and F1-2 that detect levels of DiOC6 dye were adjusted to a range between 400 - 500 mV for F1-1 and 317 mV for F1-2 depending on the cell line used in each experiment. The percentage of cells that exhibit low levels of DiOC6 uptake reflects loss of mitochondrial membrane potential and apoptosis.

### **2.10 Annexin V-FITC Analysis**

In this assay, once apoptotic responses are confirmed using DiOC6, annexin V analysis allows one to distinguish between early and late apoptosis. The early stage of apoptosis is detected when the membrane phospholipid phosphatidylserine (PS) is translocated from the inner leaflet of the plasma membrane to the outer leaflet and exposes PS to the external environment. Annexin V is a calcium dependant phospho-lipid binding protein and has a high affinity for PS. As described in the protocol, certain calcium and salt concentrations are required to allow binding of annexin. In order to identify cells bound to annexin, a fluorescent stain is used, specifically, fluorescein isothiocyanite (green fluorescence). Each sample of cells is harvested at a density of  $1 \times 10^6$ , and transferred from 6 or 9 well plates (Nunclon Surface) to 1.5 ml microfuge tubes (ISC Bioexpress) and centrifuged using a Labnet z cytopspin (Hermle) for five minutes at 15 rpm, and then aspirated. The pellet of cells was washed with PBS (solution must be adjusted to a pH of 7.2 and autoclaved). 1 L of PBS contains 1.44 grams of  $\text{Na}_2\text{HPO}_4 \cdot 7\text{H}_2\text{O}$ , 8 grams of NaCl, 0.24 grams of  $\text{KH}_2\text{PO}_4$ , and 0.2 grams of KCl. Washes in PBS were repeated two or three times, repeating the same procedure. PBS is then removed and the cell pellet was resuspended in 500 ul of the annexin binding buffer (500 ml of binding buffer contains 10 mM of HEPES/NaOH that has a pH of 7.4, 140 mM of NaCl, and 2.5 mM  $\text{CaCl}_2$ ). Finally,

100  $\mu$ L of the cells in binding buffer were transferred to 5 ml Falcon snap cap, polystyrene tubes.

This was followed by the addition of 5  $\mu$ L of annexin V-FITC (BD Biosciences) to the Falcon tube along with 10  $\mu$ L of propidium iodide stock (Sigma Aldrich). 20 ml of propidium iodide stock for annexin V analysis contains 50  $\mu$ g of propidium iodide in 20 ml of 1x PBS. The Falcon polystyrene tubes were incubated in a 37°C/5% CO<sub>2</sub> incubator in the dark for approximately 15 minutes. The final volume of samples in the polystyrene tubes was adjusted to 500  $\mu$ L by adding 400  $\mu$ L of annexin binding buffer to the incubated polystyrene tubes. For annexin V analysis, Facscan from Becton Dickinson was used along with Cell Quest software version 4.1 x. The channels that were adjusted and correspond to green and red fluorescence F1-1 and F1-3 were adjusted to 217-300 mV and 350-400 mV, respectively. F1-3 corresponds to propidium iodide stained cells; whereas, Annexin V stain corresponds to F1-1.

### **2.11 Cell Cycle Analysis**

Changes in cell cycle may provide further insight into the mechanism involved in apoptosis when cells are exposed to different reagents and can be measured either directly or indirectly. In most of the direct assays, the time course for changes in DNA and synthesis of DNA is measured. One direct method of identifying cell proliferation is through incorporation of propidium iodide (Sigma Aldrich), a standard cytometric fluorescence used to measure DNA content over a time course. Propidium Iodide was used in annexin analysis above; however, in this case other ingredients were added to form propidium iodide solution for cell cycle analysis. For each condition subjected to cell cycle

analysis, 500  $\mu$ L of cells (cell density  $5 - 5.3 \times 10^5$ /ml) were treated for approximately 8 hours with desired reagents (UCN-01, lovastatin, fluvastatin, and simvastatin either alone or in combination). The cells were then pelleted at 1500 rpm, 4° C using the Jouan, Model CT 4 22 and resuspended in 1.5 ml PBS followed by addition of 3 ml of 67% ethanol and incubated at 4°C for an hour. After centrifugation, the samples were aspirated and the pellet was resuspended in 1.0 ml propidium iodide solution (20 ml of propidium iodide or propidium iodide solution contained  $3.8 \times 10^{-3}$  Na citrate to neutralize the acid, 0.5 mg/ml RNase, and 0.01 propidium iodide).

The resulting sample was analyzed by flow cytometry using the Becton Dickinson Facscan and Cell Quest software as previously mentioned. The plot of F1-3 (channel detecting red fluorescence) was set to approximately 217 – 300 mV. Cells stained with red fluorescence indicate increase in DNA synthesis or changes in DNA compared to untreated cells. For graphing the cell cycle data obtained from Cell Quest, curves were adjusted manually using Modfit LT 2.0 software (Verity). In this analysis, data files were converted to graphs showing peaks corresponding to S, G2/M, and G1 phases of the cell cycle.

## **2.12 DNA Fragmentation**

One major indication of apoptosis is the cleavage of chromosomal DNA at the nucleosomal sites and is marked by fragmentation that occur at weights approximately 200 base pairs. Annexin V analysis, morphological analysis, and DNA fragmentation correlate in showing apoptosis (5). For this assay cells were at a density of  $20 \times 10^5$  cells/ml for each sample, the cell density was confirmed using the coulter Z2 particle analyzer. In this case, a marker that marks every 100 bp is used (Invitrogen 10748-010). The cell samples were

centrifuged at 1500 rpm for 10 minutes at 4° C (Jouan, Model CT 4 22) and the pellet was resuspended in Gibco medium (see section 2.1 for contents). Then 450 uL of the lysis buffer was added to the suspension (2 ml of lysis buffer consists of: 5 mM Tris-base from BioRad, 20mM EDTA, 0.5 % TritonX-100 (with a pH of 8), and 100 ug/ml Proteinase K). The 1ml solution containing cells and lysis buffer were vortexed and transferred to 1.5 ml microfuge tubes (ISC Bioexpress USA). The samples were incubated in a water bath at 56° C for approximately 18 hours. The samples were then centrifuged in an F-20 microrotor (50,000 x g) for 45 minutes. This action separated the larger particles of the cell from the cellular species of lower weight. The supernatant was carefully removed without touching the pelleted cells at the bottom of the microfuge tube and the solution was transferred to a new 1.5 microfuge tube. RNase A (Sigma-Aldrich) was then added to the existing solution at a concentration of 200 ug RNase per 1 ml of lysis buffer/cells.

These samples were incubated for 3 hours at 37°C/5% CO<sub>2</sub>. The 1.8% agarose gel obtained from Gibco-BRL was mixed with a 500 ml volume of TBE buffer (1L of TBE buffer contains 54 grams Tris-base, 27.5 grams boric acid, 20 ml 0.5M EDTA (pH = 8.0) in 1 liter of milli Q water). The prepared agarose was poured into a BioRad apparatus and allowed to set to form a gel before electrophoresis using a 2 mm tooth comb (BioRad) was conducted. The gel was subjected to 120 volts until the purple band (DNA marker from Invitrogen) migrated to a position 3-4 inches from the bottom of the BioRad apparatus.

### **2.13 Clonogenicity**

To evaluate colony-forming ability following drug treatment, a soft agar cloning assay was performed. Cells were briefly washed approximately three times with serum-free

1640 RPMI medium (Gibco Life Technologies, see section 2.1 for contents).

Approximately 5000-50,000 cells/condition were used and the density was adjusted using the Becton Dickinson Coulter 2Z particle size analyzer. Then a 1% agar solution in ultrapure water was prepared (agar from Invitrogen). A heat block from Fisher Scientific was used to keep the agar warm (heated to 45°C) and prepared agar solution was aliquoted to five 15 ml conical tubes. RPMI medium (Gibco Life Technologies) containing 20% FBS was then added to five more separate conical tubes. Drug treatments were washed from the treated cells using 1640 RPMI medium with 10% FBS (contents as described in section 2.1). The coulter counter/particle size analyzer to determine cell density and the density was adjusted to 5000 – 50000 cells/ml according to the Becton Dickinson 2Z Coulter counter. 1 ml of solution consisting of medium, agar and cells were added to a 12-well plate (three wells per condition) with each well containing the same cell density. The plates (Nunclon Surface Technologies) were placed in a 37°C/5% CO<sub>2</sub>, fully humidified incubator. Within the culture plates, 1 ml of ultrapure water was added between the wells to ensure that the agar remained flexible. After 10 days of incubation visible colonies of cells in agarose gel were scored using an Olympus Model CK inverted microscope (Model AX70) and colony formation for each condition was calculated in relation to values obtained for control cells (5).

#### **2.14 Western Blot Analysis**

Western blot analysis is generally used to view proteins according to weight. Approximately 10 – 15 ml of treated cells at a density of  $5-7 \times 10^5$  cells/ml were transferred to a 15 ml conical tube and pelleted using a Jouan, Model CT 4 22 centrifuge at

12,800 x g for five minutes at 4°C, the supernatant was removed/discarded and the remaining pellet was lysed by sonication (Misonix Model 2, Inc) in 1x sample buffer (2 ml of 1 x sample buffer is composed of the following: 62.5 mM Tris base (pH 6.8), 2% SDS, 50 mM dithiothreitol, 10% glycerol, 0.1% bromphenol blue, and 5 mg/ml each chymostatin, leupeptin, aprotinin, pepstatin, and soybean trypsin inhibitor (CLAPS), 1 mM each sodium vanadate, sodium pyrophosphate (Na PPI)). Following sonication, the cells lysated in sample buffer were transferred from the 15 ml tube conical tube to the 1.5 ml microfuge tubes and boiled for 5 min. The microfuge tubes containing the cells and sample buffer were centrifuged at 12,800 for 5 min in a Hermle z cytospin from Z Net. Once centrifuged, the cell samples were transferred to another 1.5 ml microfuge tube. Protein concentration for each cell sample was quantified using Coomassie Protein Assay Reagent (Pierce, Rockford, IL) (4). In this case, a Hitachi U-2000 spectrophotometer was used at a wavelength of 595 nm in order to assure equal loading of protein during electrophoresis.

For measurements taken, 1 ml of ultrapure water was distributed to cuvettes along with 1 ml of coomassie reagent, and 1 uL of sample. The absorbance exhibited by each sample was then measured using the Hitachi spectrophotometer. One cuvette containing only coomassie reagent and water was used for calibration of the instrument. Each sample was gently inverted to mix the sample and measurements were automatically recorded in ug/ul. Appropriate calculations were performed to ensure equal loading of cell samples into the BioRad pre-made SDS gels with a 4-15% Tris-HCl gradient and 15 uL volume wells (catalog number 161-1158). The pre-made gels were place into a BioRad apparatus and enough running buffer was added to cover the bottom half of the apparatus (2L of 5 x

Running Buffer stock consisted of 188 grams of glycine, 30.4 grams of tris base, and 10 grams of SDS, and adjusted to a pH of 7.6. For making 2 L of running buffer, 400 ml of stock was used and milli Q water was added to adjust the buffer volume to 2L). Finally, samples were separated by SDS-Page electrophoresis at a voltage of 120 mV for approximately for an hour and a half or until the straight purple band or marker (Invitrogen 10748-010) has reached approximately 3 inches from the bottom of the apparatus. The gel samples were then transferred onto a 0.2  $\mu$  nitrocellulose membrane (BioRad). For transferring protein from the gel to a nitrocellulose membrane, cassettes (Fisher Scientific) were soaked in transfer buffer (6 L transfer buffer contains 348 grams of glycine, 30.4 grams of tris base, and 3200 mL of methanol, and milli Q water filled to a volume of 6 L , and adjusted to a pH of 7.4). The sponge pad in the cassette was covered with filter squares (Whatman 3M filter paper) before the gel was added on top of the filter. The combs and bottom edge of the gel were removed before placing it on the filter and covering the gel with the square nitrocellulose membrane. Rollers from Fisher Scientific were used to remove air bubbles from the gap in between the gel and membrane. The cassette was placed into the BioRad transfer box already containing transfer buffer. Once four cassettes were added to the BioRad transfer box, transfer buffer was added to fill the box. The transfer box was then set to receive 400 mA for two hours.

After transfer, cassettes were removed, the gel and filter discarded, and nitrocellulose membranes were blocked with 5% milk (Carnation) in TBS-Tween 20. 2L of 10 x TBS-Tween 20 stock consisted of 24.2 grams Tris base, 80 grams NaCl, and 1 liter of milli Q water. From stock to make a 2L solution of 1 x TBS-Tween 20 200 ml of the stock

was used along with 2 ml of tween-20 and approximately 1.8 liters of ultrapure water to achieve a final volume of 2 liters. The membranes were kept in the blocking solution at room temperature for 1 hour. Then the blocking buffer was removed and the membrane was probed with the desired primary antibody (see below for the specific primary antibodies used). Before each primary antibody could be added to the membrane appropriate dilutions of primary antibody were made in 5% BSA with 1 x TBS-Tween 20 (see above for TBS-Tween 20 contents). The membrane was incubated on a Lab-Line shaker in the desired primary antibody/5% BSA in TBS-Tween 20 overnight at 4°C. The blots were then washed twice in TBS-Tween 20 for 15 minutes and then incubated with a 1:2000 dilution of horseradish peroxidase-conjugated secondary antibody (anti-mouse or rabbit) (Kirkegaard & Perry, Gaithersburg, MD) in 5% milk/TBS-Tween 20 at room temperature for 1 hour. After washing twice in TBS-Tween 20 for 15 min, the proteins were visualized via Western Blot Chemiluminescence Reagent (Perkinson and Elmer Life Science Products, Boston, MA) (4). Finally, to ensure equal loading and transfer of proteins, the blots were reprobed with antibodies against actin (Signal Transduction Laboratories) or tubulin (Calbiochem).

The following antibodies were used as primary antibodies: phospho-p38 MAPK (Thr180/Tyr182) antibody (1:1000; rabbit polyclonal; NEB); phospho-JNK (Thr183/Tyr185), JNK1, JNK2, phospho-Akt (Ser473), Akt; Cell Signaling Technology); phospho-cdc2 (Tyr15) antibody (1:1000; rabbit polyclonal; Cell Signaling Technology); anti-p21Cip/WAF1 (1:500; mouse monoclonal; Transduction Laboratories, Lexington, KY); anti-p27kip1 (1:500; mouse monoclonal; PharMingen, San Diego, CA);



antihuman Bcl-2 oncoprotein (1:2000; mouse monoclonal; DAKO, Carpinteria, CA); Bax (N-20; 1:2000; rabbit polyclonal; Santa Cruz Biotechnology Inc.); Bcl-xS/L (S-18; 1:500; 5107 rabbit polyclonal; Santa Cruz Biotechnology Inc.). Antihuman/mouse XIAP (1:500; rabbit polyclonal; R&D System, Minneapolis, MN); anti-Caspase-3 (1:1000; rabbit polyclonal; PharMingen); cleaved-Caspase-3 (*Mr* 17,000) antibody (1:1000; rabbit polyclonal; Cell Signaling Technology); anti-Caspase-9 (1:1000; rabbit polyclonal; PharMingen); anti-PARP (1:2500; mouse monoclonal; Calbiochem); and cleaved PARP (*Mr* 89,000) antibody (1:1000; rabbit polyclonal; Cell Signaling Technology).

### **2.15 Analysis of Cytosolic Cytochrome C**

Cells ( $2-3 \times 10^6$  cells/ml) were centrifuged and washed in PBS then lysed by incubating for 30 seconds in 2 mL of lysis buffer. The 2 ml of lysis buffer contains 75 mM NaCl, 8 mM  $\text{Na}_2\text{HPO}_4$ , 1 mM  $\text{NaH}_2\text{PO}_4$ , 1 mM EDTA, and 350 mg/ml digitonin. The lysates were then centrifuged at 12,000 x g for 1 minute in a Cyto-Tek centrifuge, and the supernatant was collected and added to an equal volume of 2x sample buffer. 1 ml of 2x sample buffer contains 125 mM Tris base (pH 6.8), 2% SDS, 100 mM DTT, 10% glycerol. The resulting protein samples were quantified using the same procedure described in the previous section and separated by 15% SDS-PAGE, and subjected to western blot analysis as described by the procedure in section 2.14. Anticytochrome *c* (mouse monoclonal; PharMingen) was the primary antibody used at a dilution of 1:500.

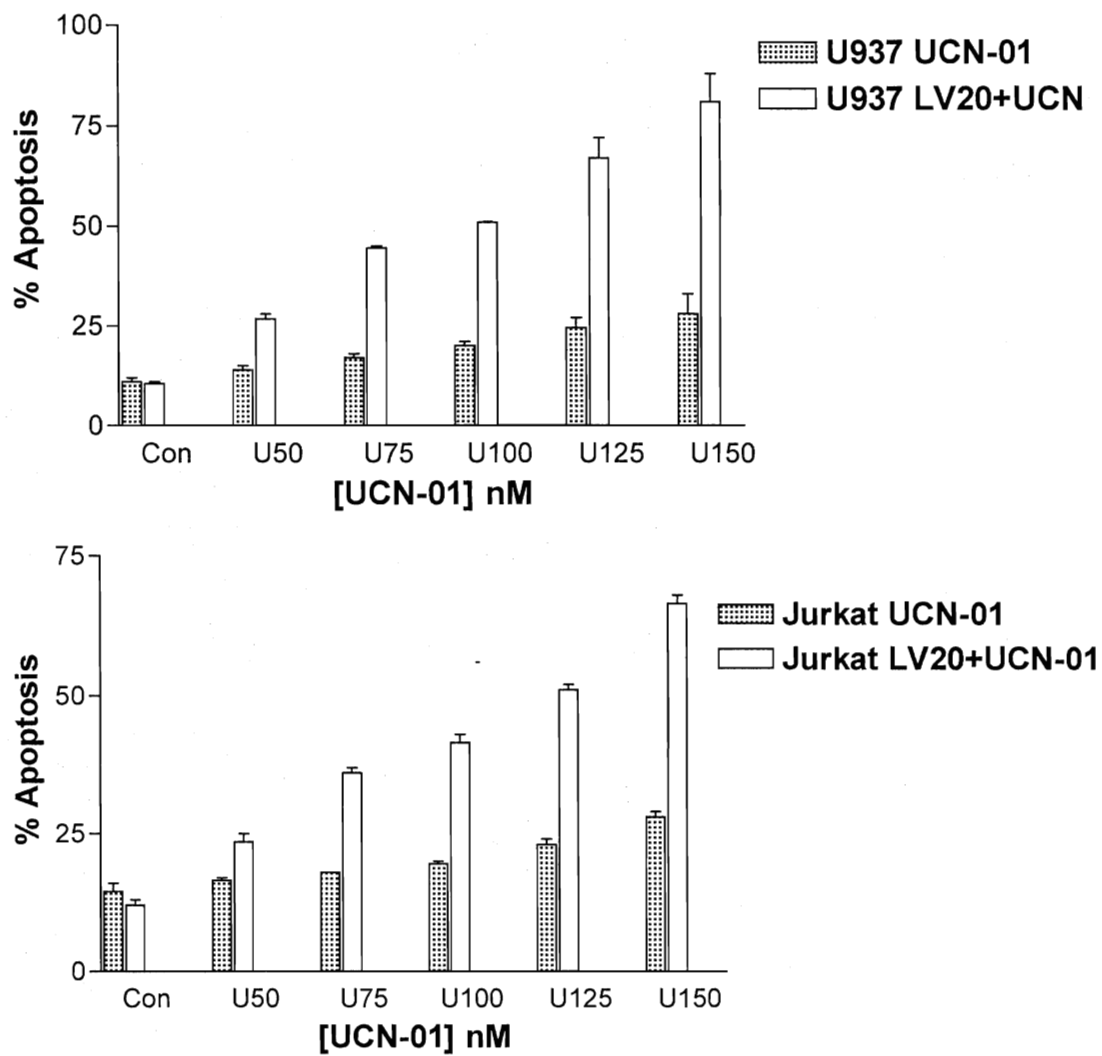
## **2.16 Statistical Analysis**

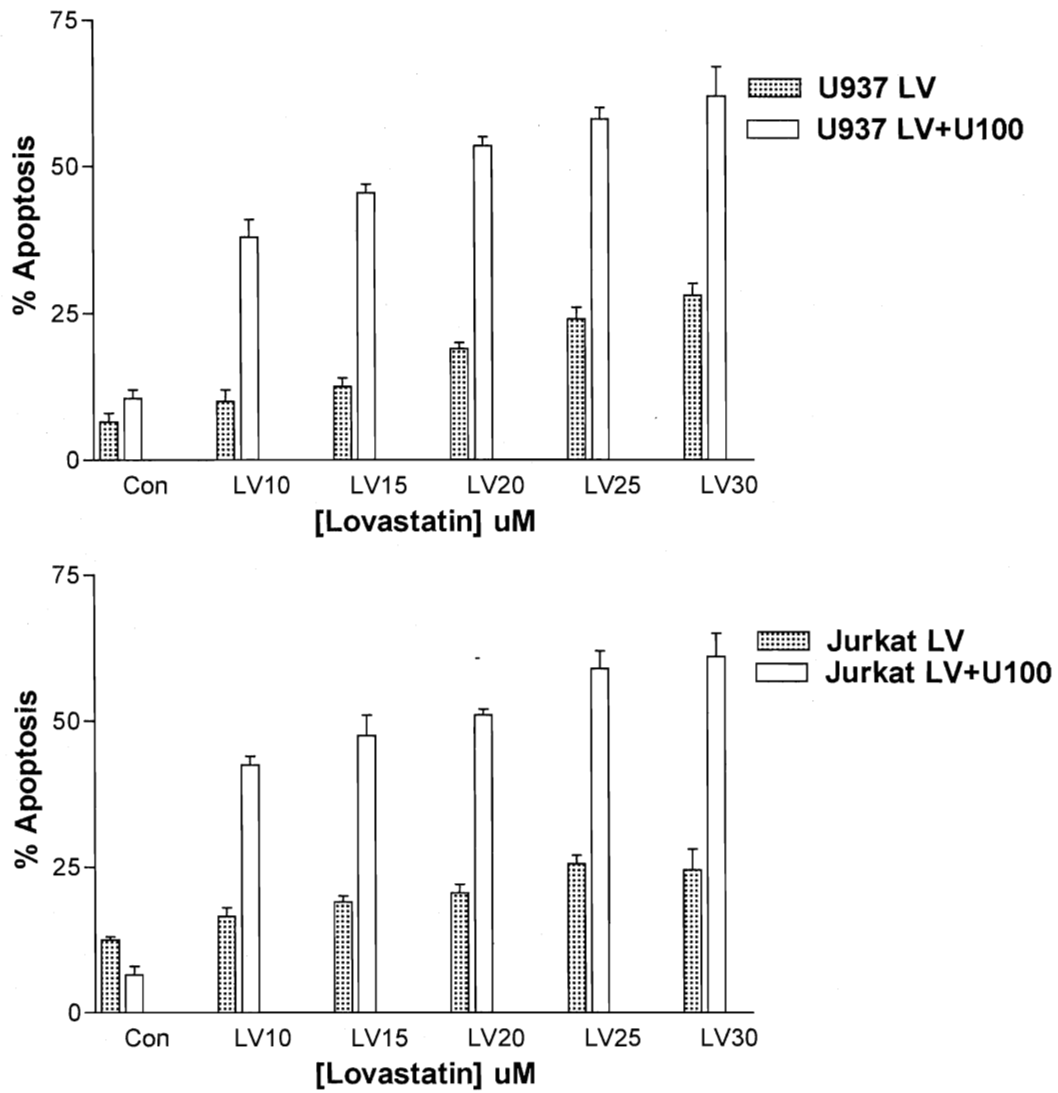
For analysis of apoptosis (morphology and Annexin V), cell viability, and colony forming ability, values represent the means  $\pm$  standard deviation for at least three separate experiments performed in triplicate. Analysis of synergism was performed according to Median Dose Effect analysis using Calcsyn and Prism software programs (Biosoft, Ferguson, MO). Statistical analysis was done using Prism Pad Software, version 3 (Biosoft, Ferguson MO) using a student's t-test at an a priori significance level of  $p \leq 0.05$ .

## Results and Data Analysis

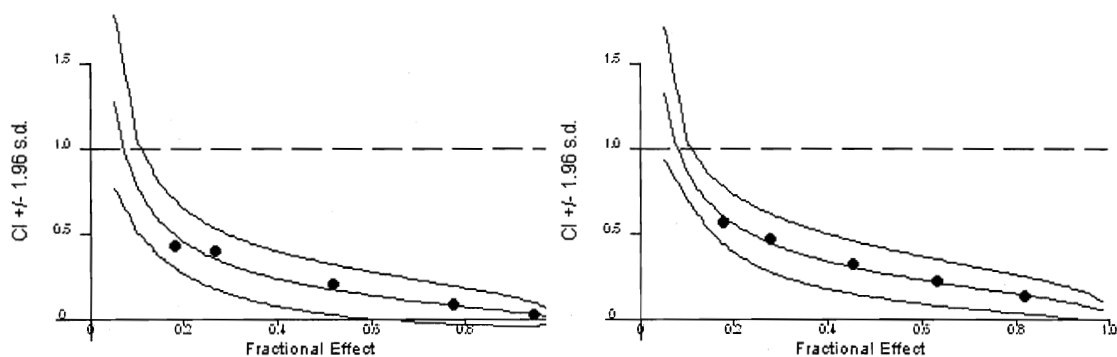
### 3.1 Co-administration of UCN-01 and Co-enzyme Reductase Inhibitors Induces a Dramatic Apoptotic Response.

In the Figure 3.1, U937 and Jurkat cells were exposed to lovastatin and UCN-01 individually over a course of 18 hours. Following treatment over 18 hours, 400 uL of cells were collected and treated to DiOC6 dye for membrane potential analysis. Apoptosis was determined by the amount of DiOC6 taken up by the cell. For consistently varying doses administered up to 150 nM of UCN-01, the degree of apoptosis shows a marked, but gradual increase compared to the control cells ( $p \leq 0.05$ ). However, when the cells were exposed to lovastatin (HMG CoenzymeA reductase inhibitor) combined with UCN-01 at lower doses there is a significant increase ( $p \leq 0.05$ ) in the amount of apoptosis to 70 % compared to cells exposed to UCN-01 alone. In Figure 3.2, there is a significant ( $p \leq 0.05$ ) increase in apoptosis compared to the control cells when treated with gradually increasing doses of lovastatin. However, cells treated with lovastatin combined with UCN-01 show a significant ( $p \leq 0.05$ ) increase compared to cells treated with lovastatin alone. As illustrated in Figure 3.3 for U937 (bottom left) and Jurkat cells (bottom right), combination indexes are lower than 1.0 indicating synergistic interactions when administering LV and UCN-01 at a constant ratio of 1000:5. The graphs below were created using Calcsyn software.

**Figure 3.1: Dose Response for U937 and Jurkat Cells (18 Hours)**

**Figure 3.2: Dose Response for U937 and Jurkat Cells (18 Hours)**

**Figure 3.3: Combination Index for Jurkat and U937 Cells**



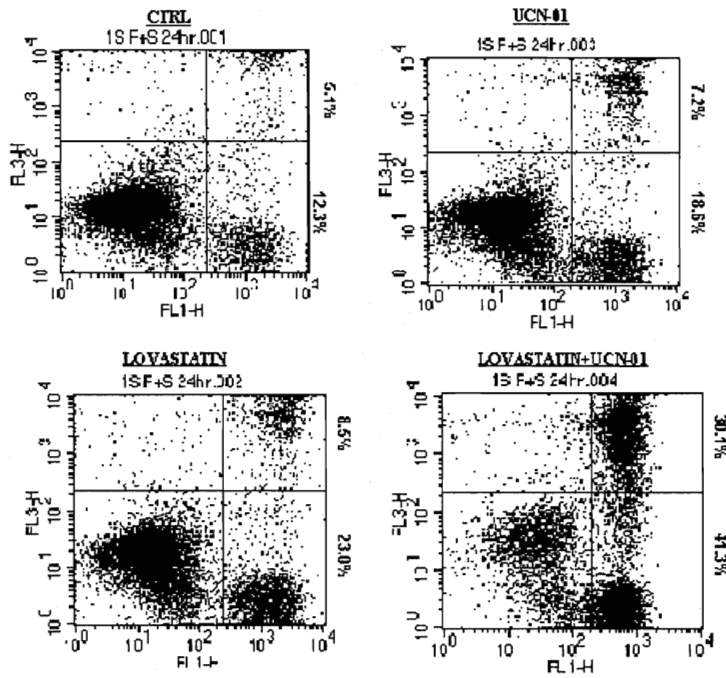
### 3.2. UCN-01 Combined with Lovastatin Induces PARP Cleavage and Caspase Activation.

The western blots in Figure 3.4 indicate that one possible mechanism by which Lovastatin and UCN-01 induce apoptosis in leukemia cells is via the intrinsic pathway as illustrated in the section I. Jurkat and U937 cells were treated with each condition as indicated for 18 hours, cells were collected and pelleted and subjected to western blot analysis as described in the materials and methods section. The data below demonstrates that UCN-01 combined with the stains tested induces caspase 3, 8, and 9 and PARP cleavage. In these studies all three forms of statins were tested and varied slightly in their potency. Once each western blot was probed with the primary antibody, all western blots were washed in TBS-Tween 20 and re-probed with actin to ensure equal loading. To differentiate between apoptosis and necrosis, further testing was done via annexin V analysis (panel A) as indicated by the PI and annexin V stained cells in the upper and lower right quadrants, respectively. Compared to the control, there is a marked shift in the

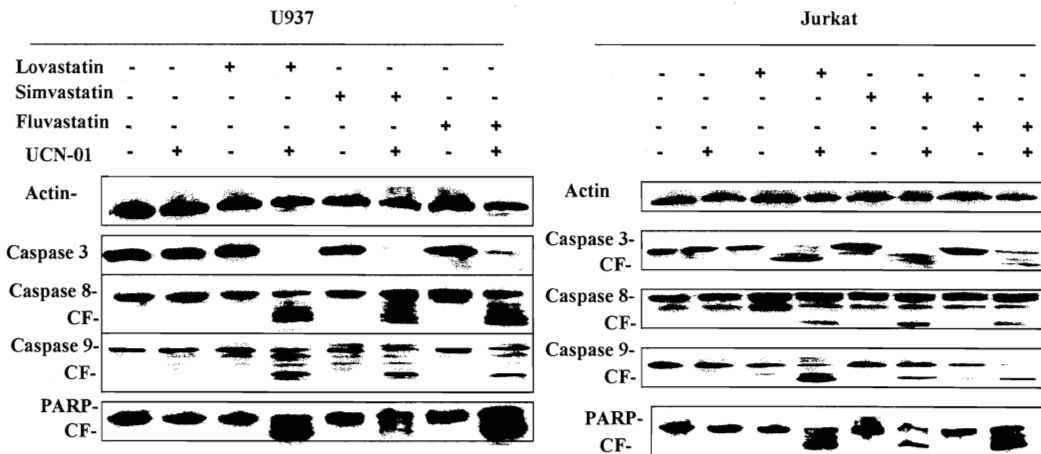
amount of cells to the upper and lower right quadrants stained with PI or annexin, indicating early and late apoptosis.

**Figure 3.4: Annexin and Western Blot Analysis**

**A.**



**B.**

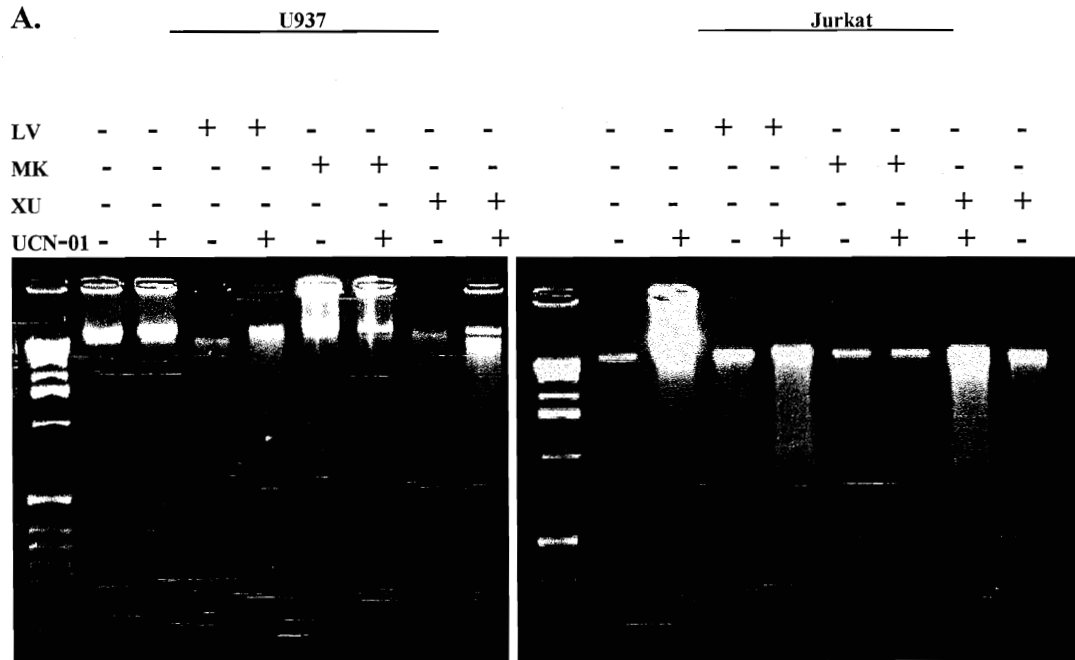


### **3.3 UCN-01/HMG-CoA Reductase Inhibitors Induces G2/M Abrogation and Changes Cell Morphology**

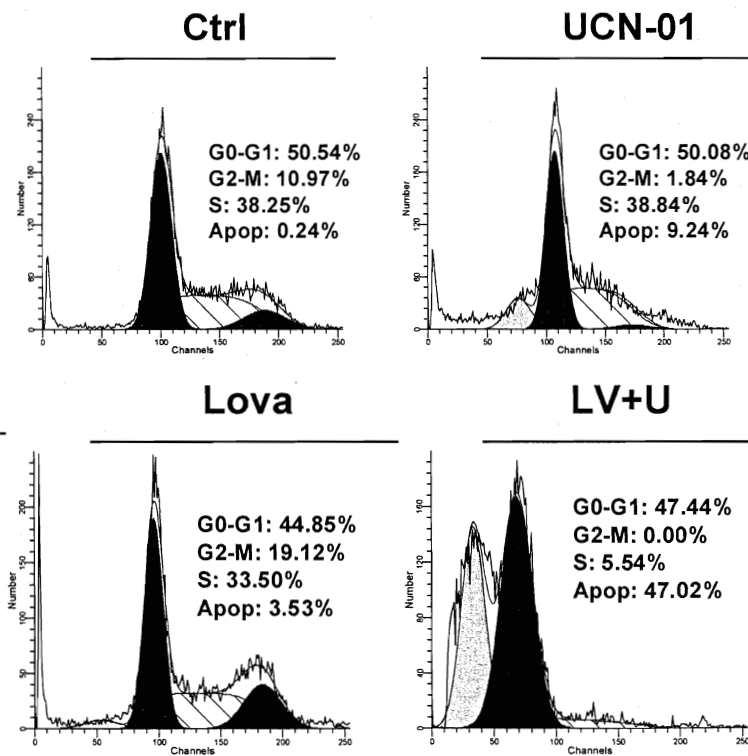
The DNA staining illustrated in Figure 3.5A was done in order assess changes in morphology and confirm apoptotic responses done during annexin staining. As mentioned previously, in the methods section, the above cells were lysed and DNA was extracted from the resulting supernatant then treated with sample buffer and separated via agarose gel electrophoresis. The gel was stained with ethidium bromide and viewed under cannon photomicroscopy. The graphs in Figure 3.5 B, demonstate that there is a marked increase of cells in the G2/M phase of the cell cycle when leukemia cells (U937) are exposed to UCN-01 or with HMG-CoenzymeA reductase inhibitors, individually. In addition, DNA analysis demonstrates dramatic apoptotic responses due to DNA damage in cells exposed to both reagents.



Figure 3.5: DNA Analysis and Cell Cycle



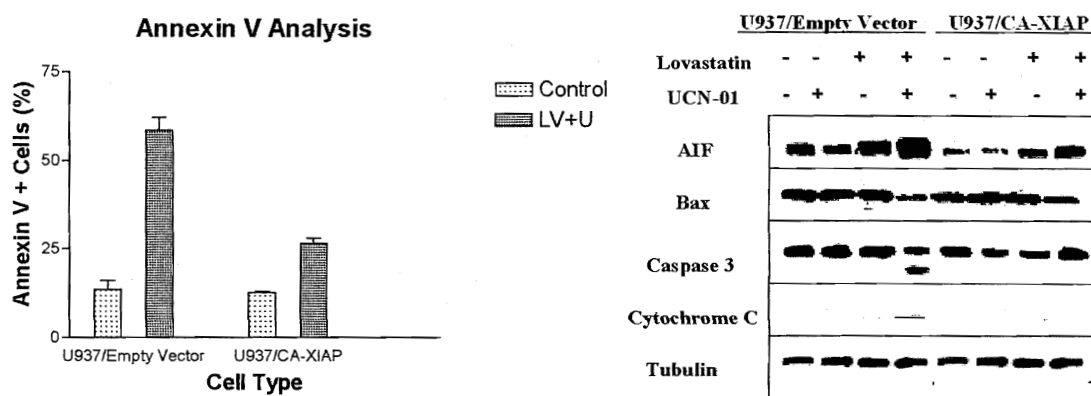
**B.**



### 3.4 UCN-01 and Lovastatin Induce Mitochondrial Membrane Damage and Induces XIAP and Caspase 3 Cleavage.

In order to further assess the exact mechanism of apoptosis and determine cytosolic distribution, leukemia cells were assessed via cytochrome *c* analysis (data not shown). Cells overexpressing U937/CA-XIAP and U937/Empty vector cells were treated with lovastatin (20  $\mu$ M)/UCN-01 (100 nM) for 18 hours and annexin V analysis was performed on untreated cells and the combination of lovastatin and UCN-01. Figure 3.6 indicates the release of cytochrome C and AIF expression when exposed to both lovastatin and UCN-01. Compared with the XIAP/Empty vector cells, U937/CA- XIAP cells indicate a significant ( $p \leq 0.05$ ) resistance to apoptosis when exposed to UCN-01/LV (18 hours).

**Figure 3.6: Western Blots and Cytochrome C Analysis**

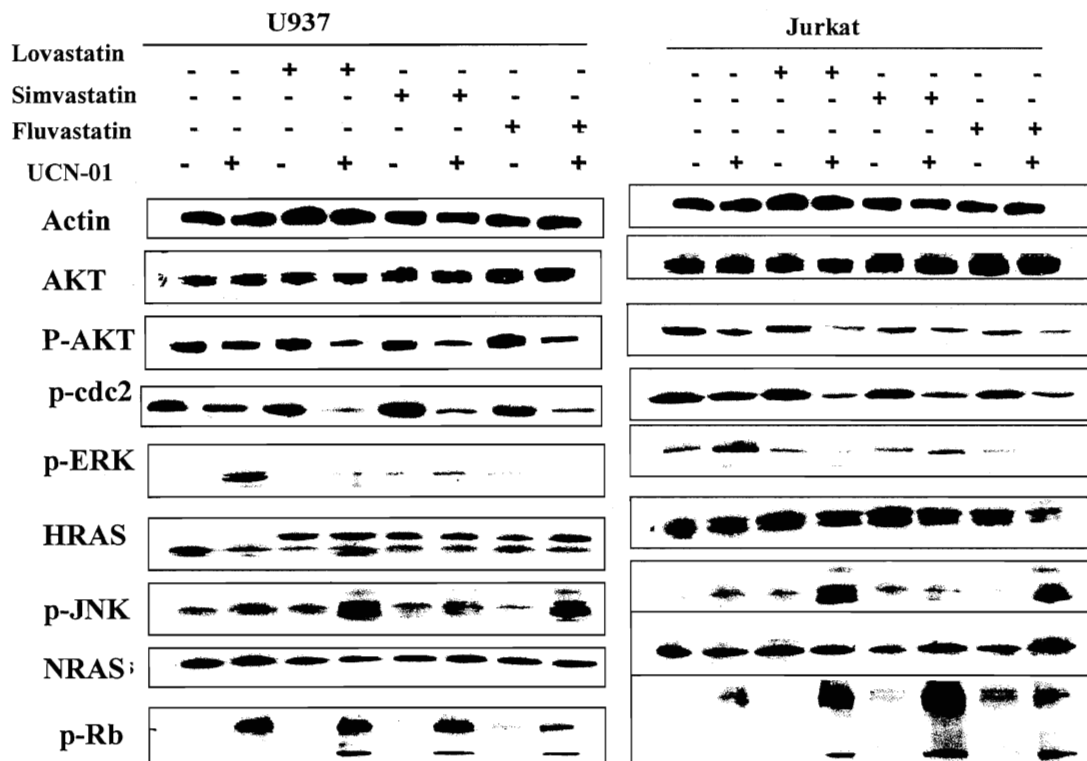


### 3.5 Lovastatin Blocks MEK/ERK Pathway Activated by UCN-01

In Figure 3.7, leukemia cells were subjected to western blot analysis. As indicated above, ERK is activated by UCN-01 documented by the strong expression of phospho-ERK when leukemia cells are exposed to UCN-01 alone and a marked increase in JNK

phosphorylation when combined with HMG CoA reductase inhibitors. However, when lovastatin is administered (lane 3), p-ERK levels are dramatically decreased compared to the amount of p-ERK expressed in the presence of UCN-01 alone. UCN-01, slightly decreased p-cdc2 expression, whereas the combination of statin/UCN-01 dramatically down-regulated of p-cdc2 phosphorylation. Finally, western blots were performed on two RAS isoforms in order to assess the dominant isoform involved in RAS inhibition. According to the blot, fluctuations in HRAS expression indicate that the unprocessed or unmodified RAS (band 6) expression increases with the addition of lovastatin, simvastatin, and fluvastatin. When lovastatin is administered in combination with UCN-01 these effects are also present.

**Figure 3.7 PI3K/AKT ad RAS/RAF/MEK/ERK Pathway**

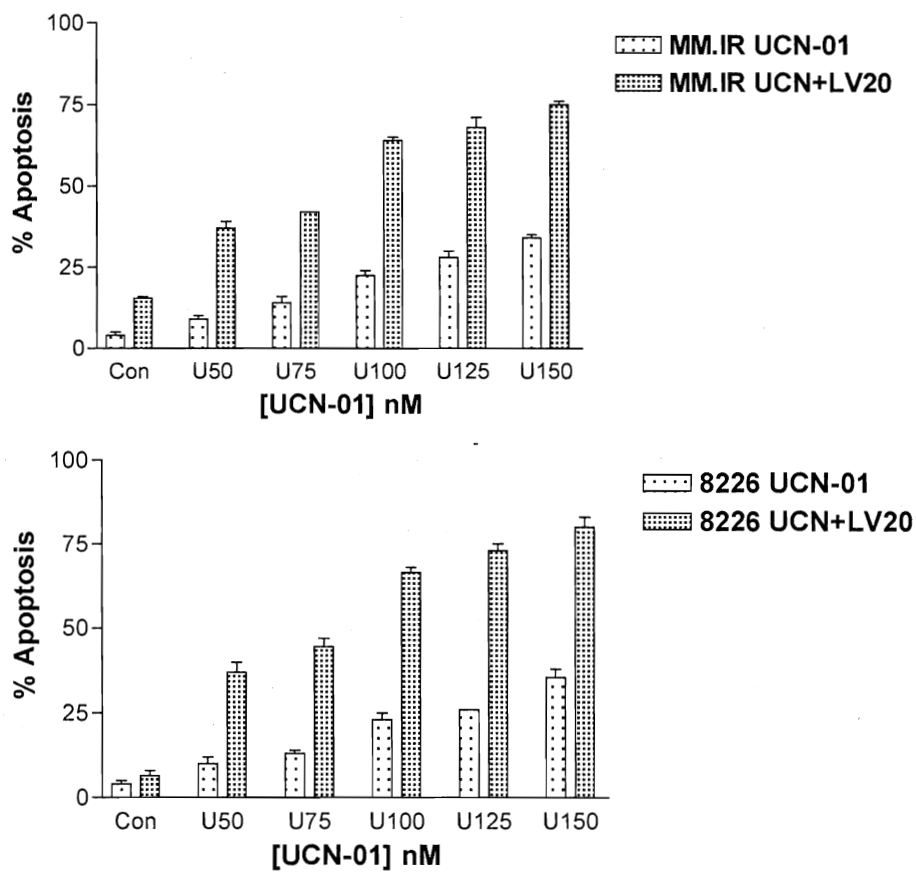


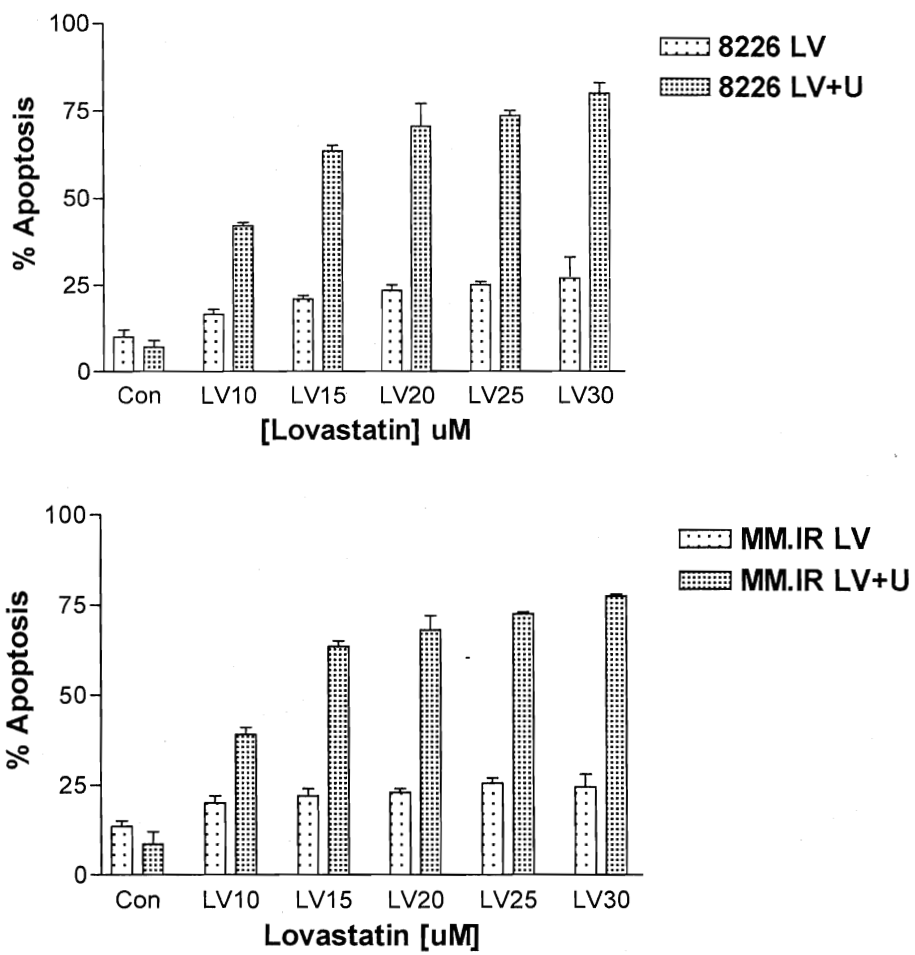
### **3.6: Myeloma Cells Show Dramatic Apoptotic Response.**

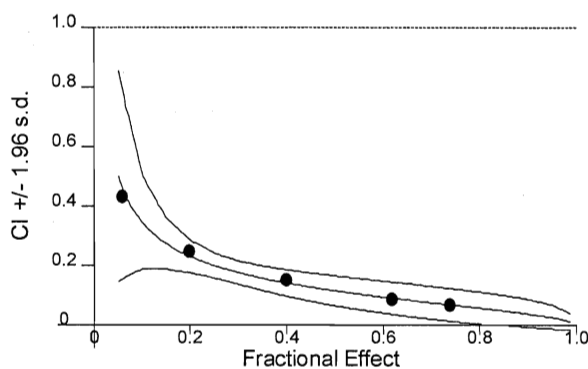
The cell lines below for 8226/Sensitive cells and MM.1R Cells were subjected to DiOC6 analysis to indicate the optimal synergistic response. Various cell lines were used in the myeloma study to observe consistent protein expression and apoptotic response. The 8226/Sensitive cell lines and MM.1R cell lines were treated with a corresponding control, single, and combination of reagents for 18 and 24 hours. Figure 3.8 demonstrates a significant ( $p \leq 0.05$ ) increase in apoptosis compared to the control cells when exposed to UCN-01 alone in 8226/Sensitive and 1R cells. In addition, Figure 3.8 illustrates a marked ( $p \leq 0.05$ ) increase in apoptosis when cells are exposed to UCN-01 combined with lovastatin compared to cells treated with UCN-01 or lovastatin alone. Figure 3.9 demonstrates a significant ( $p \leq 0.05$ ) increase in apoptosis compared to the control cells when exposed to lovastatin individually in 8226/Sensitive and 1R cells. In addition, Figure 3.9 illustrates a marked ( $p \leq 0.05$ ) increase in apoptosis when cells are exposed to UCN-01 combined with lovastatin compared to cells treated with UCN-01 or lovastatin alone. U266 cells were exposed to a 24, 36, and 48 hours in order to determine the optimal synergistic response (data not shown). It was determined that the optimal time for treatment was 18 hours for MM.1R and 8226 cell lines. The optimal synergistic response was achieved when 15  $\mu$ M of lovastatin and 100 nM of UCN-01 were administered to 8226/Sensitive cells and MM.1R cells. However, U226 cell lines were slightly more resistant and an optimal synergistic response was demonstrated at 36 hours with 10 $\mu$ M of lovastatin and 100 nM of UCN-01 (data not shown). For simvastatin, the same analysis was conducted as discussed

above and the optimal response was achieved at a combination of doses of 20  $\mu$ M of MK and 100 nM of UCN-01 (data not shown).

**Figure 3.8 Dose Response for MM.1R Cells and 8226 Cells (18 Hours)**



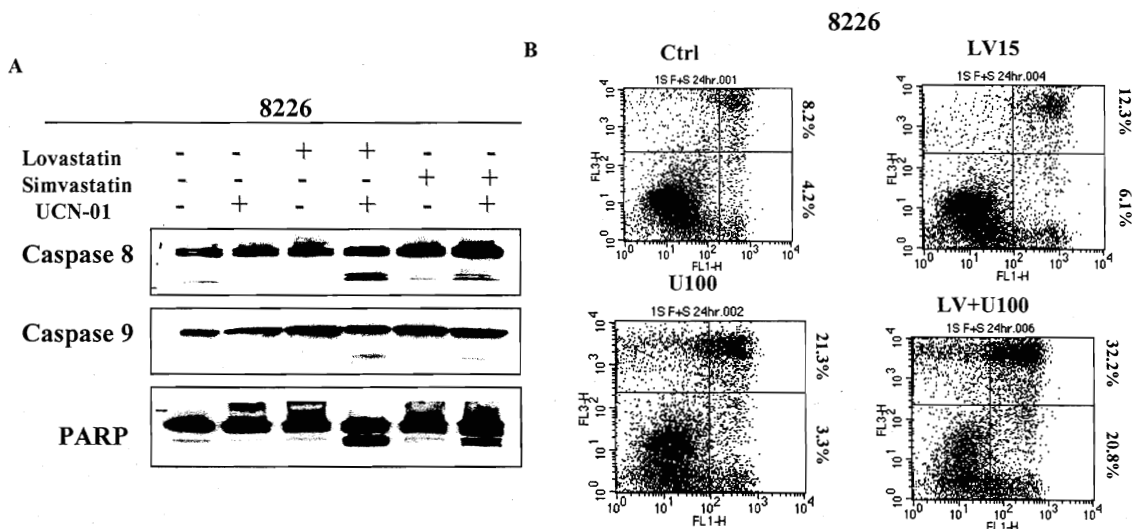
**Figure 3.9 Dose Response for MM.1R and 8226 Cells (18 Hours)**

**Figure 3.10: Combination Index for MM.1R and 8226 Cells (18 Hours)**

### 3.7 Mitochondrial Dysfunction and PARP Cleavage.

In Figure 3.11, the western blots demonstrate caspase 8 and caspase 9 cleavage consistently throughout the myeloma cell line indicating that the mechanism involved in the apoptotic response with UCN-01/statin combination causes mitochondrial dysfunction and involves the intrinsic pathway. In addition, PARP cleavage and XIAP cleavage also indicate a similar molecular mechanism to that which occurs in leukemia cells. Annexin analysis confirms apoptotic responses illustrated in preliminary DiOC6 analysis.

**Figure 3.11 Mitochondrial Dysfunction and Annexin V Analysis (8226 Cells)**



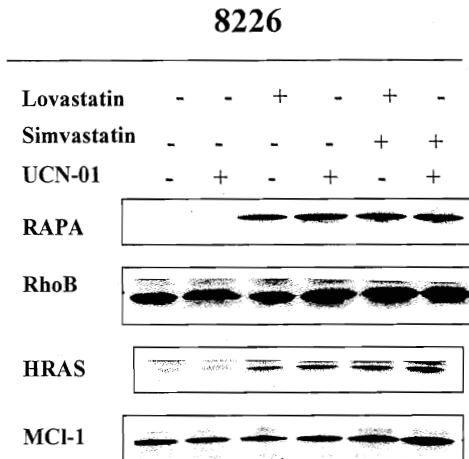
### 3.8 Inhibition of HRAS in Multiple Myeloma.

As demonstrated in Figure 3.12, inhibition of HRAS may be involved in the apoptotic response with multiple myeloma cells as seen consistently in leukemia cells. In Figure 3.12, 8226/Sensitive cells indicated a very clear expression of the unprocessed HRAS when exposed to the UCN-01/statin combination of reagents. As a result, further studies were done using U266/CA-HRAS cells in order to clearly assess that HRAS plays a predominate role in RAS inhibition in multiple myeloma. Figure 3.12 B demonstrates that U266/Empty Vector cells conferred significant ( $p \leq 0.05$ ) sensitivity compared to U266/CA-HRAS cells exposed to UCN-01 and lovastatin. Other small GTP proteins were tested to determine consistencies in protein expression among leukemia and multiple myeloma cells including Rho B and RAPA. Figure 3.12 A strongly indicates that UCN-01/lovastatin inhibit RAS processing to a mechanism similar to that demonstrated by leukemia cells.

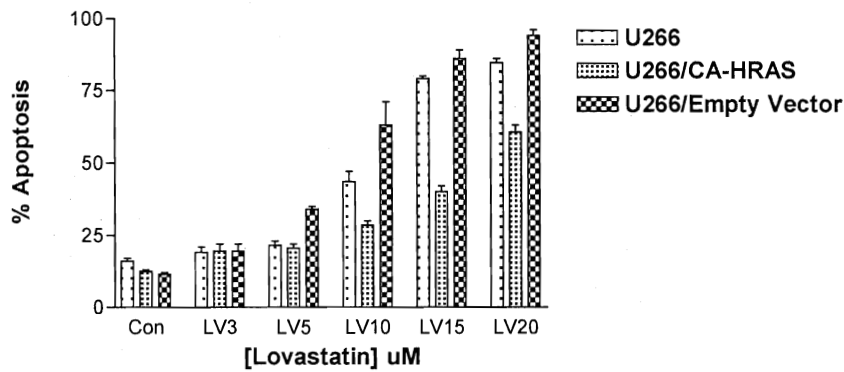


**Figure 3.12 RAS Expression in Multiple Myeloma (8226/Sensitive)**

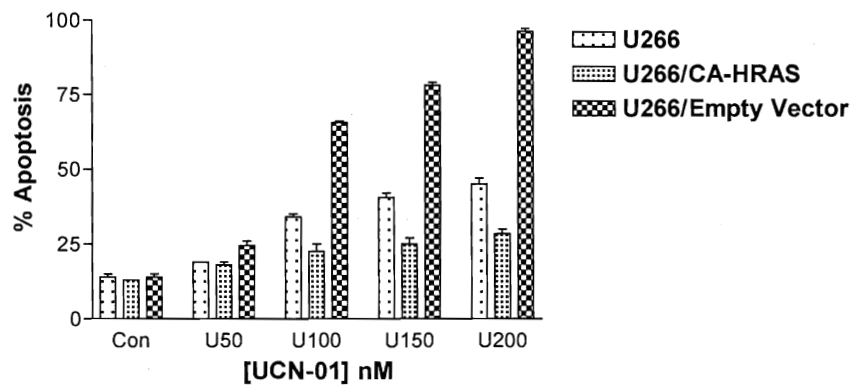
**A.**



**Dose Response (36 Hours)**



**Dose Response (36 Hours)**



## **Discussion & Conclusion**

### **4.1 Exposure of Leukemia Cells to Low Levels of UCN-01 and Lovastatin in Combination Results in Dramatic Apoptotic Response.**

In Figure 3.1 Jurkat and Leukemia cells exhibit minimal apoptotic responses when exposed to either lovastatin or UCN-01 individually. In accordance with these results, apoptosis varies from about 20% cell death to that of nearly 70% when exposed to the combination. Apoptosis was not only assessed by mitochondrial membrane potential, but confirmed via Wright-Giemsa stain preparation and annexin V analysis. Mitochondrial dysfunction indicated by DiOC6 was confirmed by cytochrome C analysis. Not only is apoptosis dramatically increased, but cell proliferation is greatly reduced compared to the control as verified by clonegenecity assays (data not shown). Compared to several clones in the control group, the number of Jurkat and U937 clones decreased dramatically (nearly 65 %) when treated by HMG CoA-reductase inhibitors/UCN-01 reagents. The degree of strength of each statin isoform varies slightly between the three forms tested with lovastatin having the greatest effect followed by simvastatin and fluvastatin.

### **4.2 UCN-01/Lovastatin Induces Apoptosis via the Mitochondrial Pathway**

Interestingly, abrogation of the G<sub>2</sub> checkpoint appears to occur preferentially in cancer cells with defective p53 tumor suppressor function. UCN-01-induced G<sub>2</sub> checkpoint abrogation has previously been shown to occur through a Cdc2-dependent pathway resulting in premature activation of this mitosis-promoting kinase in DNA-damaged cells. The molecular mechanism resulting in Cdc2 activation and G<sub>2</sub> checkpoint abrogation by

UCN-01 are not known. Increased concentration of cytochrome C in the cytoplasm results from the nucleation of a multiprotein complex known as the apoptosome. The apoptosome is comprised of the Apaf-1 adapter protein, cytochrome C, dATP, and the aspartyl-directed protease caspase 9. Cytochrome C binds to Apaf-1, and this facilitates an interaction between Apaf-1 and caspase 9. This interaction, in turn, activates the proteolytic activity of Caspase 9.

#### **4.3 Lovastatin Enhances UCN-01 Lethality Through Interruption of the RAS/RAFMEK/ERK Pathway in Leukemia and Multiple Myeloma Cells**

Because PI3K/AKT represents a major downstream target of PI3K, and has been linked, through both indirect and direct mechanisms, to a wide variety of antiapoptotic functions, it is tempting to say that lovastatin promotes the lethal effects of CDK inhibitors by blocking the activation of PI3K/AKT and one or more of its downstream targets, thereby lowering the threshold for mitochondrial damage and apoptosis. However, in the case of leukemia cells in this study it was found that while UCN-01 activated phosphorylation of ERK, activation of ERK was blocked when UCN-01 was combined with HMG CoenzymeA reductase inhibitors and was primarily responsible for enhanced apoptosis. The pathways downstream of RAS including PI3K/AKT and MEK/ERK have repeatedly been shown to promote cell survival. This phenomenon has been confirmed by previous studies in which protein kinase C and Chk1 inhibitor UCN-01 interacts in a highly synergistic manner with pharmacologic reagents targeting the MEK/ERK pathway in human leukemia and myeloma cells. Other agents, such as the Hsp90 antagonist 17-AAG, have also been shown to diminish UCN-01-induced ERK activation and potentiate

apoptosis human leukemia cells, thereby mimicking the actions of pharmacologic MEK inhibitors, such as PD98059 and U0126 (25) and HMG-CoA reductase inhibitors. Interestingly, studies done with histone deacetylase inhibitors (HDACI) and alkyllysophospholipid perifosine were associated with an increase in reactive oxygen species (ROS) production and implicated oxidative damage in HDACI/perifosine lethality. Reactive oxygen species (ROS) have a major role in the mediation of cell damage. Several defense mechanisms attempt to minimize the production and the action of harmful oxidants. Such defense mechanisms include enzymes such as superoxide dismutase, catalase, and glutathione peroxidase, as well as natural lipophilic and hydrophilic antioxidants. Excessive ROS or inhibitors of antioxidant pathways induce apoptosis. Ceramide belongs to the class of sphingolipids, cholesterol and free fatty acids. Increased levels of intracellular ceramides may either induce cell differentiation and/or apoptosis and reduced cell proliferation, initiating pro-apoptotic signaling. The relationship between the ceramide and ROS may vary with the cell type and inciting stimulus. For example, although ceramide generates ROS, increases in ROS formation can increase ceramide levels in certain cells (26). More importantly, enforced activation of PI3K/AKT or MEK/ERK blocked HDACI/perifosine-mediated ceramide generation (26). Previous studies have shown that ceramide and ROS can down-regulate PI3K/AKT through a caspase-dependent process. Conversely, ceramide blocks 3-phosphoinositide binding to the pleckstrin homology domain of PI3K/AKT. In addition, coadministration of HDACIs and perifosine failed to increase ceramide levels in cells expressing constitutively active PI3K/AKT or MEK/ERK. Together, these findings show that inactivation of both

MEK/ERK and PI3K/AKT is required for HDACI/perifosine-induced ceramide production and subsequent apoptosis. Although the above study demonstrates apoptotic mechanisms involving other pathways, the similar phenomenon among these inhibitors is the ability to interrupt the MEK/ERK and PI3K/AKT activity to induce subsequent apoptosis.

#### **4.4 Conclusions and Further Research**

The above study suggests that RAS plays a particularly important role in preventing apoptosis in leukemic cells experiencing CDK dysregulation. In addition, these and earlier studies focusing on interactions between UCN-01 and MEK1/2 inhibitors provide further evidence that leukemia cells are particularly sensitive when components of the cell cycle and survival signaling events are simultaneously disrupted. In several studies dysregulation of the PI3K/AKT pathway is associated with transformation, and there is extensive evidence that inhibitors of PI3K/AKT can enhance the lethality of present chemotherapeutics. As a result, researchers have searched for clinically relevant agents that interrupt the PI3K/AKT pathway and pathways that activate downstream targets of PI3K/AKT. Specifically, the present studies suggest that HMG- CoA reductase inhibitors, by blocking the PI3K/AKT and MEK/ERK pathway may represent useful agents to enhance the anti-tumor efficacy of agents like UCN-01. There is abundant evidence that activation of the PI3K/AKT pathway exerts antiapoptotic effects, although the mechanism(s) by which this phenomenon occurs is not entirely understood and may vary with cell type. Western blot analysis has indicated mitochondrial dysfunction and sensitivity to statin/UCN-01 reagents; however, the exact apoptotic mechanism is not clear.

Further studies are required to clarify the exact RAS isoform involved in PI3K/AKT regulation.

### Literature Cited

1. Chai J., Du C., Wu J. W., Kyin S., Wang X., Shi Y. Structural and biochemical basis of apoptotic activation by Smac/DIABLO. *Nature (Lond.)*, 406: 855-862, 2000.
2. Chan KK, Oza AM, Siu LL. The statins as anticancer agents. *Clin Cancer Res.* 2003 Jan;9(1):10-9. Review.
3. Chang F, Lee JT, Navolanic PM, Steelman LS, Shelton JG, Blalock WL, Franklin RA, McCubrey JA. Involvement of PI3K/Akt pathway in cell cycle progression, apoptosis, and neoplastic transformation: a target for cancer chemotherapy. *Leukemia.* 2003 Mar;17(3):590-603. Review.
4. Chauhan D., Pandey P., Ogata A., Teoh G., Krett N., Halgren R., Rosen S., Kufe D., Kharbanda S., Anderson K. Cytochrome c-dependent and -independent induction of apoptosis in multiple myeloma cells. *J. Biol. Chem.*, 272: 29995-29997, 1997.
5. Cheng EH, Wei MC, Weiler S, et al. BCL-2, BCL-X(L) sequester BH3 domain-only molecules preventing BAX- and BAK-mediated mitochondrial apoptosis. *Mol Cell.* 2001;8: 705-711.
6. Dai Y, Grant S. Cyclin-dependent kinase inhibitors. *Curr Opin Pharmacol.* 2003 Aug;3(4):362-70. Review.
7. Dai Y, Rahmani M, Pei XY, Khanna P, Han SI, Mitchell C, Dent P, Grant S. Farnesyltransferase inhibitors interact synergistically with the Chk1 inhibitor UCN-01 to induce apoptosis in human leukemia cells through interruption of both Akt and MEK/ERK pathways and activation of SEK1/JNK. *Blood.* 2005 Feb 15;105(4):1706-16. 2004 Oct 19.
8. Dai Y, Yu C, Singh V, Tang L, Wang Z, McInistry R, Dent P, Grant S. Pharmacological inhibitors of the mitogen-activated protein kinase (MAPK) kinase/MAPK cascade interact synergistically with UCN-01 to induce mitochondrial dysfunction and apoptosis in human leukemia cells. *Cancer Res.* 2001 Jul 1;61(13):5106-15.
9. Davies S. P., Reddy H., Caivano M., Cohen P. Specificity and mechanism of action of some commonly used protein kinase inhibitors. *Biochem. J.*, 351: 95-105, 2000.

10. Decker RH, Dai Y, Grant S. The cyclin-dependent kinase inhibitor flavopiridol induces apoptosis in human leukemia cells (U937) through the mitochondrial rather than the receptor-mediated pathway. *Cell Death Differ.* 2001 Jul;8(7):715-24.
11. Derijard B, Raingeaud J, Barrett T, et al. Independent human MAP-kinase signal transduction pathways defined by MEK and MKK isoforms. *Science.* 1995;267: 682-685.
12. Huang S, Shu L, Dilling MB, Easton J, Harwood FC, Ichijo H, and Houghton PJ (2003) Sustained activation of the JNK cascade and rapamycin-induced apoptosis are suppressed by p53/p21(Cip1). *11: 1491-1501.*
13. Jia W, Yu C, Rahmani M, Krystal G, Sausville EA, Dent P, Grant S. Synergistic antileukemic interactions between 17-AAG and UCN-01 involve interruption of RAF/MEK-and AKT-related pathways. *Blood.* 2003 Sep 1;102(5):1824-32. 2003 May 8.
14. Johnstone RW, Ruefli AA, and Lowe SW (2002) Apoptosis: a link between cancer genetics and chemotherapy. *Cell* 108: 153-164.
15. Hsu J, Shi Y, Krajewski S, et al The AKT kinase is activated in multiple myeloma tumor cells. *Blood,* 98: 2853-5, 2001.
16. Kawakami K, Futami H, Takahara J, Yamaguchi K. UCN-01, 7-hydroxyl-staurosporine, inhibits kinase activity of cyclin-dependent kinases and reduces the phosphorylation of the retinoblastoma susceptibility gene product in A549 human lung cancer cell line. *Biochem Biophys Res Commun.* 1996;219:778-783.
17. Kim K, Fisher MJ, Xu S-Q, and El-Deiry WS (2000) Molecular determinants of response to TRAIL in killing of normal and cancer cells. *Clin Cancer Res* 6: 335-346.
18. King K. L., Cidlowski J. A. Cell cycle and apoptosis: common pathways to life and death. *J. Cell. Biochem.,* 58: 175-180, 1995.
19. Kitada S, Zapata JM, Andreeff M, Reed JC. Protein kinase inhibitors flavopiridol and 7-hydroxy-staurosporine down-regulate antiapoptosis proteins in B-cell chronic lymphocytic leukemia. *Blood.* 2000 Jul 15;96(2):393-7.



20. Lam L, Cao Y. Statins and their roles in cancer. *Timely Top Med Cardiovasc Dis.* 2005 Sep 1;9:E23.
21. Leppa S., Bohmann D. Diverse functions of JNK signaling and c-Jun in stress response and apoptosis. *Oncogene*, 18: 6158-6162, 1999.
22. Macdonald SG, Crews CM, Wu L, et al. Reconstitution of the RAF-1-MEK-ERK signal transduction pathway in vitro. *Mol Cell Biol.* 1993;13: 6615-6620.
23. Milella M, Precupanu CM, Gregorj C, Ricciardi MR, Petrucci MT, Kornblau SM, Tafuri A, Andreeff M. Beyond single pathway inhibition: MEK inhibitors as a platform for the development of pharmacological combinations with synergistic anti-leukemic effects. *Curr Pharm Des.* 2005;11(21):2779-95. Review.
24. Petak I, Houghton JA. Shared pathways: death receptors and cytotoxic drugs in cancer therapy. *Pathol Oncol Res.* 2001;7(2):95-106. Review.
25. Pumiglia K. M., Decker S. J. Cell cycle arrest mediated by the MEK/mitogen-activated protein kinase pathway. *Proc. Natl. Acad. Sci. USA*, 94: 448-452, 1997.
26. Rahmani M, Yu C, Reese E, Ahmed W, Hirsch K, Dent P, and Grant S (2003) Inhibition of PI-3 kinase sensitizes human leukemic cells to histone deacetylase inhibitor-mediated apoptosis through p44/42 MAP kinase inactivation and abrogation of p21(CIP1/WAF1) induction rather than AKT inhibition. *Oncogene* 22: 6231-6242.
27. Sausville EA, Arbuck SG, Messmann R, et al. Phase I trial of 72-hour continuous infusion UCN-01 in patients with refractory neoplasms. *J Clin Oncol.* 2001;19: 2319-2333.
28. Shao RG, Shimizu T, Pommier Y. 7-Hydroxystaurosporine (UCN-01) induces apoptosis in human colon carcinoma and leukemia cells independently of p53. *Exp Cell Res.* 1997 Aug 1;234(2):388-97.
29. Shi Z, Azuma A, Sampath D, Li YX, Huang P, Plunkett W. Phase arrest by nucleosides analogues and abrogation of survival without cell cycle progression by hydroxystaurosporine. *Cancer Res.* 2001 Feb 1;61(3):1065-72.
30. Senderowicz AM. Inhibitors of cyclin-dependent kinase modulators for cancer therapy. *Prog Drug Res.* 2005;63:183-206.

31. Senderowicz AM. Development of cyclin-dependent kinase modulators as novel therapeutic approaches for hematological malignancies. *Leukemia*. 2001 Jan;15(1):1-9. Review.
32. Tournier C, Hess P, Yang DD, Xu J, Turner TK, Nimmual A, Bar-Sagi D, Jones SN, Flavell RA, and Davis RJ (2000) Requirement of JNK for stress-induced activation of the cytochrome c-mediated death pathway. *Science (Wash DC)* 288: 870-874.
33. Verheij M., Bose R., Lin X. H., Yao B., Jarvis W. D., Grant S., Birrer M. J., Szabo E., Zon L. I., Kyriakis J. M., Haimovitz-Friedman A., Fuks Z., Kolesnick R. Requirement for ceramide-initiated SAPK/JNK signaling in stress-induced apoptosis. *Nature (Lond.)*, 380: 75-79, 1996.
34. von Gise A, Lorenz P, Wellbrock C, et al. Apoptosis suppression by RAF-1 and MEK1 requires MEK- and phosphatidylinositol 3-kinase-dependent signals. *Mol Cell Biol*. 2001;21: 2324-2336.
35. Yamauchi T, Keating MJ, Plunkett W. UCN-01 (7-hydroxystaurosporine) inhibits DNA repair and increases cytotoxicity in normal lymphocytes and chronic lymphocytic leukemia lymphocytes. *Mol Cancer Ther*. 2002 Feb;1(4):287-94.
36. Yang J., Liu X., Bhalla K., Kim C. N., Ibrado A. M., Cai J., Peng T. I., Jones D. P., Wang X. Prevention of apoptosis by Bcl-2: release of cytochrome c from mitochondria blocked. *Science (Wash. DC)*, 275: 1129-1132, 1997.
37. Yu C, Wang S, Dent P, Grant S. Sequence-dependent potentiation of paclitaxel-mediated apoptosis in human leukemia cells by inhibitors of the mitogen-activated protein kinase kinase/mitogen-activated protein kinase pathway. *Mol Pharmacol*. 2001;60: 143-154.
38. Wang Q, Worland PJ, Clark JL, Carlson BA, Sausville EA. Apoptosis in 7-hydroxystaurosporine-treated T lymphoblasts correlates with activation of cyclin-dependent kinases 1 and 2. *Cell Growth Differ*. 1995 Aug;6(8):927-36. Erratum in: *Cell Growth Differ* 1995 Oct;6(10):1339.
39. Widmann C, Gibson S, Johnson GL. Caspase-dependent cleavage of signaling proteins during apoptosis. A turn-off mechanism for anti-apoptotic signals. *J Biol Chem*. 1998;273: 7141-7147

VITA**Payal Khanna**

<b>Education</b>	09/1998-05/2002	Virginia Commonwealth University	Richmond, VA
	<b>Bachelor's of Science</b>		
	Major: Biomedical Engineering; Minor: Physics		
	09/2002-12/2005	Virginia Commonwealth University	Richmond, VA
	<b>Master's of Science</b>		
	Major: Biomedical Engineering; Thesis: Apoptosis using HMG-CoA Reductase Inhibitors		
<b>Work experience</b>	May 2003-Present	MCV Hospitals/VCU	Richmond, VA
	<b>Graduate Student</b>		
	Techniques/training in Western Blotting, transfection of cell lines, maintenance of leukemia and myeloma cell lines, flow cytometry, immunoblotting		
	Involved apoptotic studies of leukemia and Myeloma cell lines including Jurkat and U937 cell lines when exposed to various chemotherapies.		
	Sept. 2001-May 2002	MCV Hospitals/VCU	Richmond, VA
	<b>Senior Design Studio/Undergraduate Project</b>		
	Aim was to design a bioreactor that allows cells to seed onto a polymer scaffold and design an apparatus/method to allow cells to proliferate and mechanically condition cells to form a strong vessel.		
	Tested the strength of the vessel as a result of pressure and performed mechanical strengthening tests using MTS of the resulting artificial GRAFT.		
	August 2000-September 2002	PMUSA Research Park	Richmond, VA
	<b>Intern/Research Assistant</b>		
	Assisted researchers and graduate/PhD students in the field of Nano-sized metallics.		
	Weekly presentations to corporation on research conducted.		
	Filtration research to reduce harmful constituents in industrial pollution such as carbon monoxide. Included researching properties of Nanoparticles and working with a particle size analyzer and zeta potential.		
	Composition analysis was done using a microbalance, calorimetric system, and extended experimentation using various surfaces in a laboratory setting.		
<b>Patents and publications</b>	<u>Dai Y, Rahmani M, Pei XY, Khanna P, Han SJ, Mitchell C, Dent P, Grant S., Blood.</u>		
	"Farnesyltransferase inhibitors interact synergistically with the Chk1 inhibitor UCN-01 to induce apoptosis in human leukemia cells through interruption of both Akt and MEK/ERK pathways and activation of SEK1/JNK." Feb. 2005.		